# DIFFUSION-CONTROLLED BUBBLE GROWTH

S. G. Bankoff

Department of Chemical Engineering
Northwestern University, Evanston, Illinois



## I. Introduction

In a previous article (B8), the subject of diffusion-controlled phase change, subject to two provisos, was reviewed in some detail. These constraints were the following: (1) the motion must be induced solely by the phase change; and (2) the diffusion and pressure equations must be, within a negligible error, uncoupled. The latter restriction implies that forces and accelerations

need not be considered in formulating the differential equation or the boundary conditions for the diffusion problem. In theory, at least, this latter restriction is not applicable to rapid vaporization processes. In particular, the study of diffusive bubble growth processes, with which this article is concerned, adds an extra dimension of complexity over those situations studied heretofore. It is not only necessary to consider the convective motion, resulting from the large change in density upon vaporization, in the diffusion equation, but also separately to consider the equation of motion, since inertial, surface tension, and viscous effects may be appreciable. In practice, however, diffusion effects control in the late, or asymptotic, stage of bubble growth, and most theoretical effort to date has centered upon an understanding of this simpler case. Fortunately, the asymptotic solutions are applicable, with small error, during most of the lifetime of the visible bubble, so that principal interest for process application centers upon them. These theories will, therefore, be reviewed in some detail, since they represent important specializations of the general theory of diffusion-limited phase change.

Nevertheless, although bubble formation and growth play an important role in the mechanics of boiling heat transfer, solid–liquid reactions with gas evolution (including electrolysis), cavitation (with its associated degradation of propulsion and pumping characteristics), and effervescence (precipitation of gas bubbles from a supersaturated solution), present applications of bubble dynamics theory are quite limited. The theory deals with the spherically symmetric growth of a single bubble in a large body of liquid at rest at infinity. In actual practice, bubbles nearly always originate as microscopic bits of gas or vapor entrapped in small crevices on a solid surface. Often the solid surface is large in extent compared to the bubble diameter, so that departure from spherical (or hemispherical) flow symmetry is frequently significant. Turbulence, bubble interaction, bubble coalescence, and translational velocity of the fluid with respect to the bubble are other complicating factors. It is necessary, therefore, to consider phenomenological theories for various aspects of bubble behavior; since these are less well founded in experiment, while *a priori* error estimates cannot be obtained, these will be only briefly reviewed.

Not only is theoretical analysis in this field difficult, but also experimental measurements of the velocity and temperature fields surrounding a bubble are at the limit of present capabilities, because of the small length and time scales involved. This lack of information, together with the uncertainty introduced by the presence of the solid wall, make comparison of theory with experiment difficult. The status of experimental information on bubble growth rates is, therefore, briefly reviewed. Finally, a number of special topics, including bubble nucleation, are touched upon. Some general comments conclude the review.

Several recent applications hinge strongly on diffusion-controlled bubble dynamics. The self-regulating properties of water- or organic-moderated nuclear reactors depend upon a reduction in reactivity in the course of a power excursion. A portion of this reduction can be attributed to expansion of the moderator as a result of void formation. It is doubtful, however, that single-bubble growth theory can be meaningfully applied to the expulsion of moderator from heterogeneous reactors, since coalescence of bubbles to form a continuous vapor film on the hot fuel surfaces occurs rapidly. On the other hand, shutdown of the KEWB reactor, which is an experimental aqueous homogeneous reactor, during power transients is attributed to the formation of numerous radiolytic gas bubbles throughout the liquid (B26). An interesting recent application, connected with a dry photographic process, is the formation of minute gas bubbles in molten plastic as the result of decomposition of a diazo compound (B14). A major difficulty, even in these applications, is not so much an estimate of the growth rate of any particular bubble as it is an estimate of the rate of nucleation of new bubbles per unit volume. The theory of bubble nucleation is still not well understood, but it seems very likely that heterogeneous nucleation (from gas or vapor entrapped in crevices on solid surfaces) dominates over homogeneous nucleation (from statistical density fluctuations) (B2, B3, F2). This means that the nucleation characteristics, even in the absence of macroscopic solid surfaces, depend upon the suspended particle population; a systematic study of this relationship is not yet available.

The subject of diffusion-controlled bubble growth is, of course, a rather small part of the large subject of bubble dynamics, whose scope is too broad to be included in this review. Specifically excluded are cavitation bubbles, whose collapse is inertia rather than diffusion controlled, the formation and detachment of bubbles from orifices, oscillations of bubbles in a pressure field, and the challenging subject of the mechanism of nucleate boiling heat transfer, in which bubble formation and detachment must certainly play a dominant role.

## II. Spherically Symmetric Bubble Growth

### A. Formulation of the Problem

Consider the growth of a small vapor or gas bubble, far from any other body, initially in equilibrium with a large volume of stationary liquid, as a result of a small displacement from equilibrium. The bubble maintains a spherical shape because of surface tension, and the liquid motion is purely radial. Note that this does not imply that the temperature or concentration field is likewise spherically symmetric. The governing equations and boundary

and initial conditions for bubble growth have been discussed by a number of authors (P6, P7, S3, S11, S13a).

Upon integrating the continuity equation for the laminar, purely radial flow of an incompressible fluid, the liquid velocity $u$ is found to be

$$ur^2 = \mathscr{F}(t), \qquad u = u(r, t), \qquad r > R(t) \tag{1}$$

where $\mathscr{F}(t)$ is a function of time to be determined in this case from the conditions at the bubble surface $R = R(t)$. A mass balance on the bubble requires that

$$\frac{d}{dt}\left(\tfrac{4}{3}\pi R^3 \rho'\right) = 4\pi R^2 \rho[\dot{R} - u(R, t)] \tag{2}$$

where the dot denotes time differentiation and primed quantities refer to the vapor properties. The bracketed term on the right is the net velocity normal to the bubble surface, expressing the fact that the liquid at the bubble wall has a velocity slightly different from that of the wall. On the left-hand side the vapor density varies relatively slowly compared to the bubble volume, which usually increases by several orders of magnitude. Hence, it is satisfactory to consider a time-averaged vapor density $\langle \rho' \rangle$ whereupon Eqs. (1) and (2) give

$$u(R, t) = \varepsilon \dot{R}, \qquad \varepsilon = 1 - \frac{\langle \rho' \rangle}{\rho} \tag{3}$$

$$u(r, t) = \varepsilon \dot{R} R^2 r^{-2}$$

By integrating the stress equation for the radial motion of an incompressible Newtonian fluid from the bubble wall to infinity, the equation of motion for the bubble wall was obtained by Scriven (S3), upon using Eq. (3), in the form

$$R\ddot{R} + \left(2 - \frac{\varepsilon}{2}\right)\dot{R}^2 = \frac{p(R) - p_\infty}{\varepsilon \rho} - 4\nu \frac{\dot{R}}{R} \tag{4}$$

where $p_\infty$ and $p(R)$ are the pressures far from the bubble and at the bubble wall, and $\nu$ is the liquid kinematic viscosity. The pressure $p(R)$ is related to the pressure within the bubble $p_b$ by[1]

$$p_b = p(R) + \frac{2\sigma}{R} \tag{5}$$

[1] In some cases the dynamic surface tension may exceed the equilibrium value. Scriven (S4) shows that for a Newtonian surface viscosity model an extra term equal to $4\kappa \dot{R}/R^2$ should be added to the right-hand side of Eq. (5), where $\kappa$ is the effective surface-dilational viscosity.

It is now assumed that the contents of the bubble are at all times in equilibrium with the liquid at the bubble wall.[2] Plesset and Zwick (P6) show that the average bubble wall velocity (of the order of 10 cm/sec for a steam bubble at atmospheric pressure with 10°C superheat) is much less than the acoustic velocity in either liquid or vapor, so that compressibility effects can be neglected. Also, the velocity of the bubble wall is considerably less than the average velocity with which evaporating molecules stream away from the surface, given in terms of the absolute evaporation rate as $\gamma(R_g T/2\pi M)^{1/2}$, where $\gamma$ is an accommodation coefficient. The critical velocity for a water surface at 100°C is about 8 m/sec, which is appreciably higher than the mean bubble wall velocity, so that the departure from the equilibrium vapor pressure is negligibly small. For organic liquids, whose accommodation coefficients are thought to be higher than those of water (W4), this neglect is even better justified. Finally, because of the relatively large thermal diffusivity of the vapor, temperature gradients within the bubble may be neglected under most circumstances. In water vapor at atmospheric pressure the characteristic diffusion length $(2\alpha' t)^{1/2}$ is 0.24 cm for $t = 0.01$ sec, at which time the bubble radius for 10°C superheat is about 0.1 cm. For all but the fastest-growing vapor bubbles, therefore, the assumption of thermodynamic equilibrium between the vapor and the bubble wall liquid is justified, and

$$p_b = p_g + p_v \tag{6}$$

where $p_g$ is the inert gas partial pressure and $p_v$ is the vapor pressure of the liquid at the bubble wall. The equations of motion finally become

$$\frac{p(R) - p_\infty}{\varepsilon\rho} = \frac{p_v + p_g - p_\infty - 2\sigma/R}{\varepsilon\rho} = R\ddot{R} + \left(2 - \frac{\varepsilon}{2}\right)\dot{R}^2 + 4\nu\frac{\dot{R}}{R} \tag{7}$$

Normally the viscous term is negligibly small (Z5), and $\varepsilon \sim 1$. In this case the equation reduces to the extension of the potential flow (Rayleigh) equation (L4), given by Plesset (P3), taking surface tension into account.

The energy equation, assuming spherical symmetry, constant thermal properties, and negligible viscous dissipation, becomes

$$\frac{\partial T}{\partial t} = \alpha\left(\frac{\partial^2 T}{\partial r^2} + \frac{2}{r}\frac{\partial T}{\partial r}\right) - \frac{\varepsilon\dot{R}R^2}{r^2}\frac{\partial T}{\partial r} + \frac{Q}{\rho c_p} \tag{8}$$

where $Q$, the volume rate of heat release, may be a function of both space and time. Similarly, in a multicomponent mixture, assuming constant mass density and diffusivity, a mass diffusion equation for one of the components (taken

[2] This is not true in the final stages of collapse of cavitation bubbles, which are not diffusion limited.

to be the more volatile component in a two-component mixture) is

$$\frac{\partial C_A}{\partial t} = \mathscr{D}\left(\frac{\partial^2 C_A}{\partial r^2} + \frac{2}{r}\frac{\partial C_A}{\partial r}\right) - \frac{\varepsilon \dot{R} R^2}{r^2}\frac{\partial C_A}{\partial r} + Q' \tag{9}$$

where $Q'$ represents the instantaneous local rate of concentration increase due to the presence of distributed mass sources. For $t < 0$, the bubble is in equilibrium with the surrounding liquid, so that

$$R(0) = \frac{2\sigma}{p_{v0} + p_g - p_\infty} + \delta_1 \tag{10}$$

where $\delta_1$ represents a small displacement from the equilibrium bubble radius (S3). Alternatively, the initial displacement from equilibrium may be considered to be caused by a weak volume heat source (P7). The asymptotic growth rate is not affected by the details of the initial displacement, providing that it is small. What is affected is the waiting time for the surface tension and inertial effects to be relaxed. The initial temperature and concentration are specified functions of position:

$$T(\mathbf{r}, 0) = g(\mathbf{r}) \tag{11}$$

$$C_A(\mathbf{r}, 0) = h(\mathbf{r}) \tag{12}$$

where $\mathbf{r}$ is the radius vector. Equating the rate of increase of the mass of the more volatile component $A$ in the bubble to the convective and diffusive flux across the bubble surface gives

$$\frac{d}{dt}(y_A \rho' R) = (1 - \varepsilon)\dot{R} C_A(R, t) + \mathscr{D}\frac{\partial C_A(R, t)}{\partial r} \tag{13}$$

where $y_A$ is the mass fraction of $A$ in the vapor. Similarly, the heat balance at the bubble wall, neglecting small terms, requires that

$$\frac{d}{dt}(\rho' R \bar{L}) = k\frac{\partial T(R, t)}{\partial r} \tag{14}$$

where $\bar{L}$ represents the average heat of vaporization per unit mass of volatile material in the bubble, evaluated at the bubble wall temperature. Finally, the specification of a boundedness condition at infinity and the requirement that the bubble contents be at all times in equilibrium with the liquid at the bubble wall complete the statement of the problem. Note that the equilibrium requirement implies the absence of concentration and temperature gradients within the bubble at all times, and the uniformity of concentration and temperature, at any instant, over the entire bubble surface. This requirement applies even when the initial temperature and concentration fields in the liquid are not spherically symmetric.

When put into dimensionless form, the full problem involves eight or more dimensionless parameters, whose magnitude must be examined for any particular problem before deciding which terms can be safely neglected. This question is discussed in detail by Langlois (L5) with reference to isothermal gas bubble growth. For example, the effect of inert (nondiffusant) gas in the initial bubble is neglected hereafter; however, in the early stages of bubble growth it plays a significant role, as discussed by Dergarabedian (D2, D3), Ma and Wang (M1), and Lienhard (L7). The complete set of equations is obviously quite formidable, and it is instructive to consider first the simplest case. This involves a single diffusant from an initially uniform liquid.

## B. Asymptotic Growth of a Vapor Bubble in an Initially Uniformly Superheated One-Component Liquid

### 1. *Self-Similar (Exact) Solutions*

During the asymptotic growth stage, viscous and inertial effects are negligible. Likewise, the partial pressure of the small inert gas residue becomes negligible compared to the vapor partial pressure within the bubble. Hence, the equation of motion (4) reduces to the statement that the bubble is in mechanical equilibrium with its surroundings, and, to an excellent degree of approximation, the internal bubble pressure is equal to the ambient pressure. The growth is then strictly diffusion controlled, so that the solution developed by Kirkaldy (K4) for spherically symmetric phase growth where a density change is involved is applicable.[3] The difficulty is that it is necessary to extend the asymptotic stage all the way back to zero radius, which does not agree with the physical facts. The bubble actually begins at some finite, nonzero radius; and the inertial and surface tension terms are appreciable during the early stage of bubble growth. The exact solution, therefore, deals with an associated problem, which it is hoped closely approximates asymptotically the solution of the complete problem. The approximation error can only be determined by other methods.

In 1958, Kirkaldy (K4) published a self-similar solution for the growth, limited by the diffusion of heat or mass, of slabs, cylinders, or spheres of initially negligible size from a large body of surrounding quiescent fluid of

[3] This paper has been generally overlooked by workers in the bubble dynamics field largely because Kirkaldy was concerned with exact solutions for the growth of ice particles, and was, in fact, principally concerned with establishing the validity of the quasi-steady approximation in this problem. However, his solution is correct for spherical symmetry in one, two, or three dimensions, with convection induced by the phase change, and hence would be applicable to the growth of plane or cylindrical bubbles, as well as spherical bubbles. A summary of this analysis is given in (B8).

initially uniform concentration or temperature, where the densities of the two phases are constant but not necessarily equal. Nearly simultaneously, Birkhoff, Margulies, and Horning (B19) published the same solution for a growing vapor or gas bubble, and explored in some detail the nature of the solution. In 1959, Scriven (S3, S4) rederived this solution and extended it to two-component systems. Specializing Kirkaldy's results (B8) to the case of a bubble growing from zero radius in an initially superheated liquid containing no heat sources, the temperature distribution in the liquid is

$$\theta = \frac{\Phi_3(\eta)}{\Phi_3(\beta)}, \qquad \theta = \frac{T - T_\infty}{T_s - T_\infty} \tag{15}$$

where $T_s$ and $T_\infty$ are the saturation temperature and the temperature far from the bubble, and where the growth function for spherical symmetry in three dimensions is

$$\Phi_3(\eta) = \int_\eta^\infty z^{-2} \exp\left(\frac{-\beta^3 \varepsilon}{2z} - \frac{z^2}{4}\right) dz \tag{16}$$

Here $\eta$ is the Boltzmann (B21) transformation variable $r/(\alpha t)^{1/2}$. To evaluate the growth constant $\beta$, where $R = \beta(\alpha t)^{1/2}$, use is made of the heat balance at the bubble wall, Eq. (14), where, from Eq. (15),

$$\frac{\partial T(R, t)}{\partial r} = \frac{(T_s - T_\infty)\Phi_3'(\beta)}{(\alpha t)^{1/2}\Phi_3(\beta)}, \qquad \Phi_3'(\eta) = \frac{d\Phi_3}{d\eta} \tag{17}$$

Hence $\beta$ is the real root of

$$\frac{N_J}{\beta} \equiv \frac{\rho c_p (T_\infty - T_s)}{\beta \rho' \bar{L}} = -\frac{\Phi_3(\beta)}{2\Phi_3'(\beta)} = \chi(\beta) \tag{18}$$

where $N_J$, termed by Savic (S1) the Jakob number, may be thought of as a dimensionless driving force for bubble growth. Birkhoff, Margulies, and Horning (B19) present plots of the temperature distribution [Eq. (15)] (Fig. 1), as well as the growth function $\chi$ (Fig. 2). It is seen that $\beta > 5$ corresponds approximately to $N_J > 2.5$, giving a rough criterion for the validity of the zero-order thin thermal boundary layer assumption, to be discussed in detail later. In particular, it is shown that (B19) for $\varepsilon = 0$

$$\lim_{\beta \to \infty} \frac{N_J}{\beta} = \left(\frac{\pi}{12}\right)^{1/2} \tag{19}$$

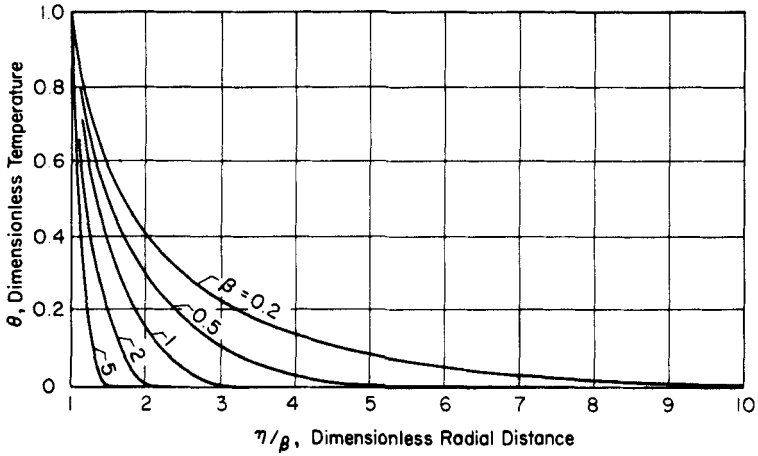


FIG. 1. Temperature profiles; $\theta(\eta)$ vs $(\eta/\beta)$ curves for different growth constants (B19).

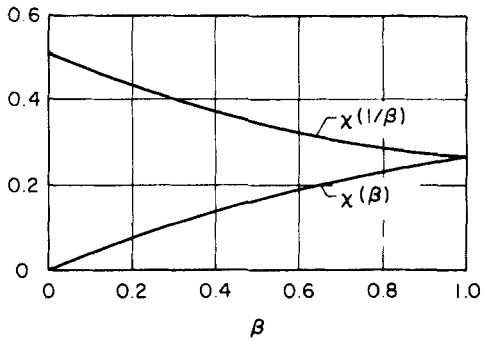


FIG. 2. $\chi(\beta)$ and $\chi(1/\beta)$ vs $\beta$, for $0 \leqslant \beta \leqslant 1$ (B19).

which implies

$$R = \left(\frac{12}{\pi}\right)^{1/2} N_J(\alpha t)^{1/2} \tag{20}$$

a result identical with the leading term of the Plesset–Zwick (P7; also B7) solutions for the asymptotic growth phase. An analogous treatment is given for the isothermal growth of a gas bubble from a uniformly supersaturated solution, for which the parameter corresponding to the Jakob number is $N_J' = (C_\infty - C_s)/C_g$. For water saturated with $N_2$ at 20°C and heated suddenly to just below the boiling point, $N_J' = 0.021$, so that the growth rate is slow (B19). For $\beta$ small, Eq. (18) gives $\beta \cong (2N_J')^{1/2}$,[4] as noted previously by Kirkaldy.

[4] There is a misprint in Eq. (26) of this reference at this point.

Birkhoff *et al.* then discuss the validity of neglecting the inertial terms in the equation of motion, Eq. (4), and conclude that it is justified if

$$R \gg \beta^2 \alpha \left[\frac{\rho}{8p(R)}\right]^{1/2} \tag{21}$$

For water boiling at 1 atm with a superheat of 1°C, the right-hand side of Eq. (21) has the value $10^{-5}$ cm, and for 10°C, $10^{-3}$ cm. Hence, the inertial terms are generally negligible in the visible bubble range, which justifies focusing attention on the asymptotic phase of bubble growth.

2. *Approximate Solutions*

The requirements for a self-similar solution of the bubble growth problem to exist are quite restrictive. In particular, the bubble must begin its growth at zero radius; inertial, viscous, and surface tension terms must be neglected at all times; and the initial temperature and/or concentration distribution in the liquid must be uniform. Actually, the bubble begins its growth at a small nonzero radius. In the early growth phase, which determines the waiting time between bubbles, or in the growth of bubbles in highly viscous polymeric media, neglect of inertial, surface tension, and viscous effects is not allowable. Further, vapor bubbles originating at a hot surface, as in nucleate boiling, grow in an environment where the temperature gradients are initially quite large, so that the assumption of uniform initial temperature cannot, in general, be made. Exact solutions of the complete equations cannot be found, so that approximate solutions of greater generality than the self-similar solution are of considerable value.

One of the earliest simplifications to be applied to the problem of the growth of diffusion-controlled vapor bubbles was the notion of a thin thermal boundary layer. This arises from the fact that at moderate pressures the volume of liquid surrounding the bubble cooled by vaporization is small compared to the volume of the bubble, in view of the large liquid to vapor density ratio. Bosnjakovic (B22) defined an effective heat transfer coefficient to the bubble, which can be estimated from a plane approximation, ignoring the effects of curvature and of stretching on the heat transfer through the boundary layer. In 1954, two different improvements of the plane approximation were published simultaneously: (*1*) a perturbation procedure by Plesset and Zwick (P7), based upon a Lagrangian formulation of the equations of motion and of heat diffusion; and (*2*) a more intuitive, although somewhat simpler, approach by Forster and Zuber (F5), based upon the notion that the moving bubble wall is equivalent to a distributed spherical heat sink expanding through a stationary medium. We begin with the Plesset–Zwick solution and its subsequent extensions, and then treat the Forster–Zuber solution and its extensions.

*a. Plesset–Zwick Perturbation Solution.* Plesset and Zwick (P6), as a preliminary to a consideration of the vapor bubble growth problem, presented a solution in successive approximations for the heat diffusion across a spherical boundary with radial motion. The approximations were based upon the notion that a thin thermal boundary layer, in which essentially all the temperature variation occurs, surrounds the bubble wall. Taking $\varepsilon = 1$, Eq. (8) becomes

$$\frac{\partial T}{\partial t} + \frac{R^2 \dot{R}}{r^2} \frac{\partial T}{\partial r} = \alpha \left( \frac{\partial^2 T}{\partial r^2} + \frac{2}{r} \frac{\partial T}{\partial r} \right) \tag{22}$$

assuming the absence of volume heat sources.

A transformation is now introduced to the new variables

$$\zeta = \int_0^t R^4(t')\, dt' \tag{23}$$

$$U = \int_0^m T_e(m', t)\, dm' + K(t), \qquad T_e = T - T_\infty \tag{24}$$

$$m = \tfrac{1}{3}[r^3 - R^3(t)] \tag{25}$$

Here $m$ is proportional to the volume of a spherical shell of liquid between the bubble wall and the radial position coordinate $r$, and hence, represents a Lagrangian coordinate, providing that a negligible volume of liquid is vaporized. $U$ is therefore a measure of the heat content of the spherical shell, to within an arbitrary additive function of time, $K(t)$; alternatively, it may be viewed as a temperature potential function. In terms of the new coordinates the diffusion equation becomes

$$\frac{r^4}{R^4} \frac{\partial^2 U}{\partial m^2} - \frac{1}{\alpha} \frac{\partial U}{\partial \zeta} = 0 \tag{26}$$

where the arbitrary additive function of time has been chosen to make the right-hand side zero, and $U(m, 0) = 0$. The boundary condition at infinity is

$$\frac{\partial U(\infty, \zeta)}{\partial m} = 0 \tag{27}$$

At the bubble wall one has

$$\frac{\partial^2 U(0, \zeta)}{\partial m^2} = \frac{1}{R^2} \frac{\partial T(R)}{\partial r} = F(\zeta) \tag{28}$$

a function of time to be determined from a heat balance on the bubble.

Noting that

$$\frac{r^4}{R^4} = \left(1 + \frac{3m}{R^3}\right)^{4/3} = 1 + \frac{4m}{R^3} + 2\left(\frac{m}{R^3}\right)^2 - \cdots \tag{29}$$

for $(3m/R^3) < 1$, and, letting $U = U_0 + U_1 + \cdots$, Eq. (26) can be written

$$\left(1 + \frac{4m}{R^3} + \frac{2m^2}{R^6} - \cdots\right) \frac{\partial^2(U_0 + U_1 + \cdots)}{\partial m^2} - \frac{1}{\alpha} \frac{\partial(U_0 + U_1 + \cdots)}{\partial \zeta} = 0 \tag{30}$$

The zero-order approximation is then given by

$$\frac{\partial^2 U_0}{\partial m^2} - \frac{1}{\alpha} \frac{\partial U_0}{\partial \zeta} = 0 \tag{31}$$

subject to the initial and boundary conditions

$$U_0(m, 0) = \frac{\partial U_0(\infty, 0)}{\partial m} = 0; \qquad \frac{\partial^2 U_0(0, \zeta)}{\partial m^2} = F(\zeta) \tag{32}$$

The solution to this linear boundary value problem is obtained by Laplace transformation, yielding for the zero-order estimate of the bubble wall temperature

$$T_0(0, t) - T_\infty = -\left(\frac{\alpha}{\pi}\right)^{1/2} \int_0^t \frac{R^2(x)(\partial T/\partial r)_{r=R(x)}}{\left\{\int_x^t R^4(z)\, dz\right\}^{1/2}} dx \tag{33}$$

Note that the effect of a spatially uniform heat source can be added directly to this expression. If the variations in $R(t)$ are sufficiently small, Eq. (33) simplifies to

$$T_0(0, t) - T_\infty = -\left(\frac{\alpha}{\pi}\right)^{1/2} \int_0^t \frac{(\partial T/\partial r)_{r=R(x)}}{(t - x)^{1/2}} dx \tag{34}$$

corresponding to the plane approximation obtained by neglecting the curvature of the boundary.

The first-order correction, from Eq. (30), satisfies

$$\frac{\partial^2 U_1}{\partial m^2} - \frac{1}{\alpha} \frac{\partial U_1}{\partial \zeta} = -\frac{4m}{R^3} \frac{\partial^2 U_0}{\partial m^2} \tag{35}$$

where the inhomogeneous term on the right-hand side may be treated as a known function. The initial and boundary conditions are homogeneous:

$$U_1(m, 0) = \frac{\partial U_1(\infty, \zeta)}{\partial m} = \frac{\partial^2 U_1(0, \zeta)}{\partial m^2} = 0 \tag{36}$$

This correction term is obtained as a convolution integral, and bounds obtained by the mean-value theorem.

Plesset and Zwick (P7) then substitute the zero-order temperature solution [Eq. (33)] into the equation of motion [Eq. (4)] to obtain the bubble radius and internal pressure as a function of time. In a sense theirs is still the only complete solution to the problem of a bubble growing from the critical (equilibrium) radius. The solution is obtained in several stages, by expansions for $(R/R_0 - 1)$ small and large, and for intermediate values, where $R_0$ is the initial bubble radius (Z6). These solutions are patched together by appropriate matching conditions to give a solution whose error can be shown to be small at every stage, provided that the thin thermal boundary layer assumption is valid. Our present concern, however, is only with the asymptotic stage, which encompasses the visible range of bubble radii for the usual liquids. The pressure of the vapor at the bubble wall may be approximated by a linear function of temperature,

$$\frac{p(R) - p_\infty}{\rho} = A(T - T_s) \tag{37}$$

Assuming negligible inert gas pressure in the bubble, $\varepsilon = 1$, and negligible viscous effects, Eq. (7) can be rewritten[5]

$$\frac{1}{2R^2\dot{R}}\frac{d}{dt}(R^3\dot{R}^2) = A(T - T_\infty) + \frac{2\sigma}{\rho R_0}\left(1 - \frac{R_0}{R}\right) \tag{38a}$$

where, from Eqs. (10) and (37),

$$2\sigma/\rho R_0 = A(T_\infty - T_s) \tag{38b}$$

In terms of the variables

$$R^* = R^3/{R_0}^3 \tag{39a}$$

$$\zeta^* = \frac{K_1}{{R_0}^4}\int_0^t R^4(t')\,dt' \tag{39b}$$

$$K_1 = (2\sigma/\rho {R_0}^3)^{1/2} \tag{39c}$$

this equation becomes

$$\frac{1}{6\dot{R}^*}\frac{d}{d\zeta^*}(R^{*7/3}\dot{R}^{*2}) = 1 - \frac{1}{R^{*1/3}} - K_2\int_0^{\zeta^*}\frac{\dot{R}^*(z)\,dz}{(\zeta^* - z)^{1/2}}, \tag{40}$$

where

$$\dot{R}^* = \frac{dR^*}{d\zeta^*}, \quad K_2 = \frac{AL\rho'}{3kR_0K_1}\left(\frac{\alpha}{\pi K_1}\right)^{1/2} \tag{41}$$

[5] Eq. (15) of the reference has a misprint at this point.

For $R \gg R_0$, the solution is obtained by taking the solution to be of the form

$$R^*(\zeta^*) = 1, \quad 0 < \zeta^* \leqslant \zeta_1^* \tag{42a}$$

$$R^*(\zeta^*) \sim \frac{2}{\pi K_2}(\zeta^* - \zeta_0^*)^{1/2} \left\{1 + \frac{b_1}{(\zeta^* - \zeta_0^*)^{1/6}} + \cdots + \frac{b_5}{(\zeta^* - \zeta_0^*)^{5/6}} + \frac{b_6 \ln(\zeta^* - \zeta_0^*)}{(\zeta^* - \zeta_0^*)}\right\},$$

$$\zeta^* > \zeta_1^* \tag{42b}$$

where $\zeta_1^*$ represents a delay time determined by the requirement from Eq. (42a) that $R^*(\zeta_1^*) = 1$, and $\zeta_0^*$ is available for matching the asymptotic solution to the preceding phase of bubble growth.

Upon matching coefficients of corresponding powers of $(\zeta^* - \zeta_0^*)$, the leading terms in the asymptotic solutions are found to be of the form

$$R \sim R_0 \left(\frac{2}{\pi K_2}\right)\left(\frac{K_1 t}{3}\right)^{1/2} \{1 + O(t^{-1/2})\}$$

$$= \left(\frac{12}{\pi}\right)^{1/2} \frac{k(T_\infty - T_s)}{L\rho'} \left(\frac{t}{\alpha}\right)^{1/2} \{1 + O(t^{-1/2})\} \tag{43}$$

$$(T - T_\infty) \sim -\frac{\alpha^2 {R_0}^2}{A} \{1 + O(t^{-1/2})\} \tag{44}$$

The predicted radius-time curves agree well (Fig. 3) with the data of Dergarabedian (D2, D3) on the asymptotic growth of vapor bubbles in water and $CCl_4$ superheated at atmospheric pressure by radiant energy. Note, in contrast to the self-similar solutions, that the bubble radius grows as the square root of time only to the order of the leading term of the asymptotic expansion. For the smallest measured radii ($\sim$0.01 cm), the error in neglecting the remaining terms in Eq. (42b) was less than 10%. To this error must be added the error due to neglecting the first-order temperature correction [Eq. (35)], estimated also to be less than 10%. Both of these errors decrease rapidly as the bubble continues to grow.

*b. Extensions of the Plesset–Zwick Method.* (1). *Iteration-perturbation method.* In the Plesset–Zwick analysis the boundary condition for the heat diffusion problem is obtained by equating the heat conducted from the liquid to the increase in enthalpy of the bubble contents, which depends upon the unknown bubble volume. This leads to an implicit nonlinear integrodiffer-

ential equation for the bubble radius, so that even the calculation of the first-order correction poses considerable difficulties. Bankoff and Mikesell (B10) noted that in the asymptotic stage the bubble wall temperature may be taken, with small error, to be equal to the saturation temperature at the ambient pressure. The replacement of the heat flux conditions by the temperature

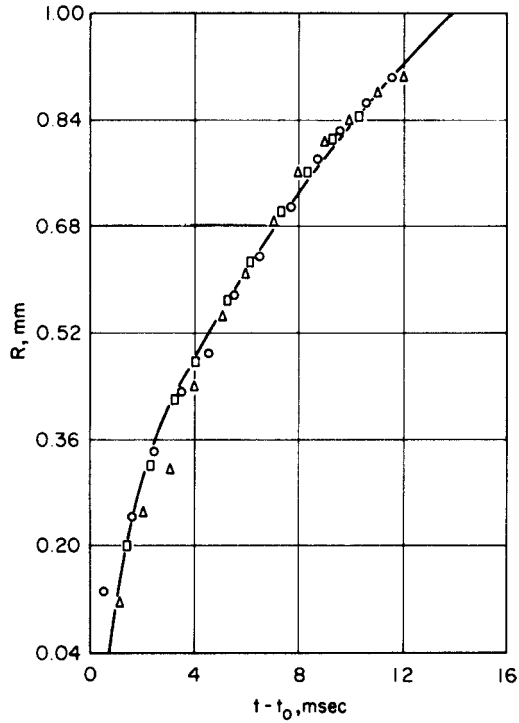


FIG. 3. Comparison of theoretical radius-time values with three sets of experimental values obtained (D2) in water superheated to 104.5°C at an external pressure of 1 atm (P7).

condition at the bubble wall was later made part of a consistent approximation scheme (B7) by introducing a second series of approximations (which was shown to converge very rapidly) to the bubble pressure, based upon the notion that the inertial and surface tension terms in the equation of motion [Eq. (7)] are small. As a preliminary, Eq. (7) can be written in terms of the variables given by Eqs. (23–25), neglecting the difference between $\varepsilon$ and unity, and also the viscous term

$$g[R(\zeta)] \equiv p_b - p_\infty = \frac{2\sigma}{R} + \rho R^4 \frac{d}{d\zeta}\left(R^4 \frac{dR}{d\zeta}\right) + \frac{3}{2}\rho R^8 \left(\frac{dR}{d\zeta}\right)^2 \qquad (45)$$

Hence, one may employ an iteration scheme which, for the zero-order perturbation, is

$$\frac{\partial^2 U_0{}^j}{\partial m^2} - \frac{1}{\alpha}\frac{\partial U_0{}^j}{\partial \zeta} = 0, \qquad j = 0, 1, \ldots; \qquad \frac{\partial U_0{}^j(m, 0)}{\partial m} = \varphi(m) \tag{46}$$

$$\frac{\partial U_0{}^j(\infty, \zeta)}{\partial m} = 0; \quad \frac{\partial U_0{}^j(0, \zeta)}{\partial m} = T_v(p^j) - T_\infty; \qquad p^0 = p_\infty \tag{47}$$

Here $U_0{}^j$ refers to the $j$th approximation to $U_0$; and $T_v(p^j)$ is the saturation temperature corresponding to the $j$th approximation of the pressure within the bubble. The heat flux condition in Eq. (14) may be integrated to give

$$R^j(\zeta) = \left[\frac{3k}{L\rho'}\int_0^\zeta \frac{\partial^2 U_0{}^j(0, z)}{\partial m^2}\, dz\right]^{1/3} \tag{48}$$

whence Eq. (45) yields

$$p^{j+1} = g[R^j(\zeta)] + p_\infty \tag{49}$$

The iteration then proceeds with this new estimate of the pressure within the bubble.

For water boiling at atmospheric pressure at a superheat of 4.5°C (D2, D3), for which inertial effects are relatively significant ($N_J = 12.0$) the surface tension and inertial correction terms are 0.012 and 0.009 atm, respectively, at the first observable datum point ($R = 0.004$ cm), and decrease very rapidly thereafter. In contrast, the ratio of the first- to the zero-order perturbation for this experiment was 3.7%. Hence, the replacement of the heat flux boundary condition by a temperature boundary condition is fully justified. In this way the zero- and first-order terms were obtained exactly, and the second-order perturbation estimated:

$$V_0 \equiv R_0{}^3 = 6N_J\left(\frac{\alpha\zeta}{\pi}\right)^{1/2} \tag{50}$$

$$V_1 = \frac{4V_0}{9N_J} \tag{51}$$

$$V_2 \doteq \frac{-5\pi V_1}{12(N_J + 4/9)} \tag{52}$$

where

$$V = R^3 = V_0 + V_1 + V_2 + \cdots \tag{53}$$

and

$$V_i = O(N_J^{-i}), \qquad i = 0, 1, 2, \cdots \tag{54}$$

The zero-order solution can be readily shown to be identical with that given by Plesset and Zwick (P7). In accordance with the observations of Birkhoff, Margulies, and Horning (B19), the perturbation procedure converges rapidly for $N_J > 2.5$.[6] Some information concerning the variation of the Jakob number with system pressure can be obtained from the data of Cichelli and Bonilla (C2), who boiled a number of organic liquids from a chromium-plated horizontal surface. For these data the excess temperature of the heating surface at maximum flux (departure from nucleate boiling) has been related to the reduced pressure by an equation of the form (B6)

$$T_w - T_s = 45 \log_{10} p_r \tag{55}$$

where $T_w$ and $T_s$ are the wall and saturation temperatures, and $p_r$ is the reduced pressure. The corresponding variation in the Jakob number with reduced pressure for two common liquids is shown in Fig. 4. As might be expected, the inertial correction term becomes entirely negligible at higher pressures, justifying the termination of the iteration scheme in Eqs. (46–49) at $j = 0$. At higher pressures, on the other hand, the perturbation series converges slowly, or possibly not at all. The application of this technique to bubble dynamics with non-isothermal initial conditions and in two-component liquids will be discussed later.

(2) *Barlow–Langlois solution of bubble growth in a viscous fluid.* Barlow and Langlois (B14) treat, in connection with a proposed dry photographic process based upon light sensitization of a diazo compound, the isothermal growth of nitrogen bubbles from a supersaturated, highly viscous, plastic melt. As a first approximation the fluid is assumed to be Newtonian in behavior. The equilibrium between the gas concentration within the bubble and the dissolved gas concentration at the bubble wall is expressed in terms of Henry's law: $C_g = k_H C(R, t)$. The diffusion equation is solved in the absence of sources of dissolved gas, which implies that the decomposition of

[6] Professor L. A. Skinner, in a private communication (S13b), makes some interesting comments, based upon Fig. 2, on the validity of the thin thermal boundary layer assumption. Approximating the curve by a straight line in the interval $0.2 < 1/\beta < \infty$, one obtains

$$\frac{\chi(1/\beta) - \chi(\infty)}{\beta} \cong -0.4$$

which, in view of Eqs. (18) and (19), can be written as

$$\beta = (12/\pi)^{1/2} N_J (1 + 0.4/N_J), \qquad \beta > 5 \quad \text{or} \quad N_J > 2.5 \tag{19'}$$

Hence, for $N_J > 4$, the error of the thin boundary layer approximation is less than 10 percent, while at $N_J = 2.5$ the error is 16 percent. The first two terms of the above perturbation solution, Eqs. (50) and (51), yield, upon inverting to the real time domain,

$$R(t) = \beta'(\alpha t)^{1/2}; \qquad \beta' = (12/\pi)^{1/2} N_J (1 + (4/9)/N_J)$$

Noting the close comparison with Eq. (19'), Skinner suggests that, in related problems which do not have exact solutions, the first-order correction will continue to be reasonably accurate.

the diazo compound upon heating the plastic is completed prior to the initiation of bubble growth. A transformation to the Lagrangian coordinates introduced by Plesset and Zwick gives, upon employing the thin boundary

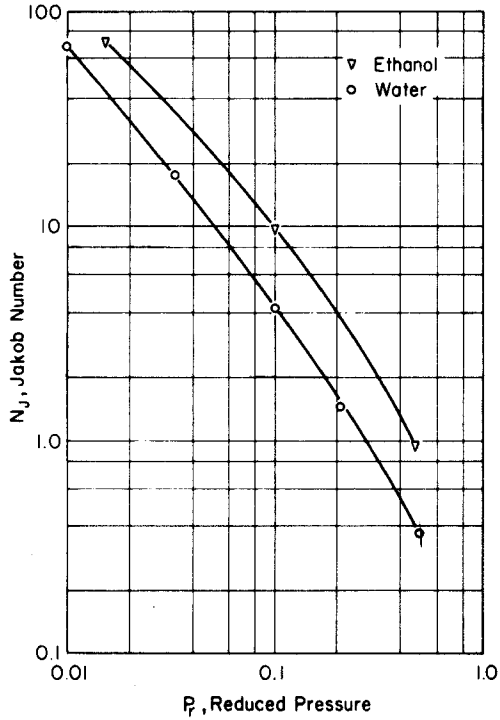


FIG. 4. Jakob number of maximum heat flux vs reduced pressure curves for ethanol and water (B7).

layer assumption (equivalent to truncating the perturbation expansion at the leading term), for the gas concentration (density) in the bubble

$$\frac{C_g}{k_H} = C_\infty - \frac{1}{3(\pi\mathscr{D})^{1/2}} \int_0^\zeta \frac{1}{(\zeta - \zeta')^{1/2}} \frac{d(R^3 C_g)}{d\zeta'} d\zeta' \tag{56}$$

which can be compared with the solution for the bubble wall temperature in the corresponding heat diffusion problem. From Eq. (7), assuming ideal gas behavior and $\varepsilon = 1$, one obtains

$$C_g = \frac{M}{R_g T} \left[ p_\infty + \rho R\ddot{R} + \frac{3}{2}\rho\dot{R}^2 + 4\mu \frac{\dot{R}}{R} + \frac{2\sigma}{R} \right] \tag{57}$$

Upon combining these equations the difficulty due to the singularity of the

integrand is avoided by taking the Cauchy principal value (H1, M8). Eventually, the integrodifferential equation

$$\frac{1}{C_\infty k_H}\int_0^t \left\{1+\left[\frac{R^3 k_H}{3}\left(\pi\mathscr{D}\int_{t'}^t R^4\,dt''\right)^{1/2}\right]\right\} C_g R^4\,dt' = \frac{2R_0{}^3 k_H}{3(\pi\mathscr{D})^{1/2}}\left[\int_0^t R^4\,dt'\right]^{1/2} + \int_0^t R^4\,dt' \quad (58)$$

is obtained, where $C_g$ is given by Eq. (57). This is obviously a formidable equation, which illustrates the complications which arise when employing a flux boundary condition at the bubble wall in solving the diffusion problem. A simpler form would be expected if a concentration boundary condition were used, in a double (perturbation–iteration) approximation series similar to that given above for the heat diffusion problem. The relation to the functional equations discussed in (B8), derived by Kolodner (K5), Boley (B20), and others for the free boundary position should also be noted. In common with all integral representations, they have the advantage of representing all features of the solution, so that limiting cases (such as $[(R/R_0)-1]$ small or large) can be derived from the same expression. Barlow and Langlois find in this way that the bubble radius initially increases linearly with time in a viscous melt. For the asymptotic stage where the bubble pressure is essentially equal to the ambient pressure, the self-similar solution of Birkhoff *et al.* can be employed. However, since the bubbles are here much smaller ($\sim 1$–$2\,\mu$) than those measured in boiling and the liquid viscosity much higher ($\sim 10^6$ dyn-sec/cm), a direct numerical solution of Eq. (58), neglecting inertial terms, is necessary over most of the range of interest. The simpler problem of the growth or collapse of a bubble where viscous and inertial effects control was previously considered by Poritsky (P8).

*c. Forster–Zuber Moving Source Solutions.* Forster and Zuber (F5) obtained an approximate solution for the heat diffusion problem by considering the moving bubble wall to be a spherical heat sink in a stationary medium. This gives the temperature at the bubble wall as

$$T_\infty - T_b = \frac{L\rho'}{\rho c_p(\pi\alpha)^{1/2}}\int_0^t \frac{R(t')\,\dot{R}(t')}{R(t)(t-t')^{1/2}} \left\{\exp\left[-\frac{[R(t)-R(t')]^2}{4\alpha(t-t')}\right] - \exp\left[-\frac{[R(t)+R(t')]^2}{4\alpha(t-t')}\right]\right\} dt' \quad (59)$$

This is equivalent to replacing the actual problem by an approximating problem, in which the heat conduction takes place in a stationary liquid,

followed by a discontinuous motion of the bubble radius from $R_0$ to an appropriate $R(t)$, where $R(t)$ is determined by the heat conducted through the bubble wall. Forster (F4) later expands this notion to a sequence of discontinuous motions and stationary heat conduction periods as an approximating procedure to any moving-boundary diffusion problem. Since the complete analytical solution must be evaluated at each point in space at each time interval, this finite-difference procedure may be lengthier than direct numerical methods.

For the asymptotic stage of bubble growth, the inertial terms of the equations of motion are neglected, and the integral in Eq. (59) is simplified by physical arguments and application of the mean-value theorem to give

$$\frac{R}{R_0} + \log\left(\frac{R - R_0}{R_1 - R_0}\right) - \frac{N_J(\pi\alpha t)^{1/2}}{R_0}, \qquad R > R_1 \tag{60}$$

$R_1$ may here be regarded as an arbitrary constant with which to match the solution to the solution for earlier times. For $R \gg R_1$, this becomes

$$\beta/N_J = (\pi)^{1/2}, \qquad \beta = R/(\alpha t)^{1/2} \tag{61}$$

which is 9% higher than the constant, $(12/\pi)^{1/2}$, of the Plesset–Zwick asymptotic solution, Eq. (43). The latter constant is also the limit for large $N_J$ of the exact solution given by Birkhoff *et al.* The Forster–Zuber theory is conceptually simpler than the Plesset–Zwick theory and may be perfectly adequate in many practical problems, although error estimates are difficult to obtain. The Plesset–Zwick theory has the advantage that the approximations are based directly upon the governing equations, so that a rigorous error estimate is available at every stage, and, in principle at least, higher-order corrections can be obtained.

Yang and Clark (Y1) have applied this source theory to two-component bubble growth problems, including the case where one of the components is a noncondensable, nonsoluble gas. An example is helium gas bubbles introduced into liquid oxygen to provide subcooling of the liquid, in order to prevent pump cavitation in liquid rocket engines. A comparison is made with the exact theory, showing reasonable agreement.

## C. Bubble Growth Under Nonuniform Initial Conditions

### 1. *Introduction*

In actual practice vapor bubbles almost always originate at solid surfaces, rather than in the midst of a large body of uniformly superheated liquid. This introduces a number of additional complications, whose effect in most cases is still largely unknown. Even for isolated bubbles the spherical shape is

usually distorted by buoyancy and inertial effects. Nevertheless, for analytical purposes it is usually assumed that the bubble retains a spherical, hemispherical, or a spherical segmental shape, depending upon the contact angle between the bubble and the solid surface. Unless this is 90°, the center of mass of the bubble translates with respect to the liquid, introducing an additional complication which is normally ignored. Furthermore, a velocity boundary layer is established around the expanding bubble in the neighborhood of the solid wall, which violates the assumption of the spherical symmetry of motion. Exact analysis of these complications has not yet proved possible. Consequently, three alternatives have been explored: (*1*) numerical solutions of the equations of change subject to suitable boundary conditions; (*2*) analytical solutions for the growth of a single bubble surrounded by a liquid of initially nonuniform temperature (where the temperature distribution is chosen to approximate the as-yet unmeasured temperature distribution in the liquid surrounding a bubble originating at a heated surface); and (*3*) alternatively, more or less heuristic theories, based upon physical arguments, which attempt to explain the main features of the process. The present section deals with the first two approaches.

## 2. *Numerical Solutions*

Once purely radial motion has been assumed, the solution can be obtained either numerically or analytically. The numerical solution has the advantage of permitting the formulation of more realistic initial and boundary conditions (although what these should be has not yet been experimentally determined). Griffith (G7) considers the growth of a hemispherical bubble on a heating surface, with initial radius $R_0 < l$, the thickness of the thermal boundary layer near the heating surface. The initial temperature distribution in the liquid near the wall is assumed to be linear through the thermal boundary layer, even in the neighborhood of the bubble wall, and constant outside this boundary layer. A numerical integration of the dimensionless energy and continuity equations is performed for various values of the parameters $N_J$ and $\omega = (T_w - T_\infty)/(T_\infty - T_b)$. Note that the thermal boundary layer next to the heated wall grows thicker as growth proceeds and that radial temperature symmetry does not exist. The temperature of the bubble wall $T_b$ is assumed to be the saturation temperature. The calculations are performed for bubble growth only. For small Jakob numbers, corresponding to large thermal boundary layers, the plane approximation is found to be inadequate. Griffith finds that for $N_J = 0.35$ a significant quantity of heat is transferred from the surface to the bubble through the liquid, while at higher values of the Jakob number, corresponding to low pressure, the bubble grows primarily as a result of vaporization of the initially superheated liquid. A further interesting result is that for small Jakob numbers the maximum size attained by the

bubble is proportional to the thickness of the layer of superheated liquid near the surface, and is independent of $N_J$.

3. *Analytical Solutions*

*a. Savic and Gosnell (S2).* Savic and Gosnell used an entirely different technique from any of those discussed above. Upon taking $\varepsilon = 1$ and $Q = 0$ (no heat source), Eq. (8) becomes

$$\frac{\partial T}{\partial t} + \frac{\dot{R}R^2}{r^2}\frac{\partial T}{\partial r} = \alpha \frac{\partial^2 T}{\partial r^2} \tag{62}$$

where it has been assumed that $(1/r)(\partial T/\partial r) \ll (\partial^2 T/\partial r^2)$. It is seen that this is tantamount to the thin thermal boundary layer assumption. Defining a new spatial variable by $y = r - R$, Eq. (62) becomes

$$\alpha \frac{\partial^2 T}{\partial y^2} + \dot{R}\frac{\partial T}{\partial y}\left[1 - \frac{1}{(1 + y/R)^2}\right] = \frac{\partial T}{\partial t} \tag{63}$$

Note that this is not a Lagrangian transformation, although the bubble wall is immobilized. The initial temperature function is taken to be a quadratic polynomial

$$t = 0: \qquad T - T_s = T_{b0} - a_1 y + a_2 y^2 \tag{64}$$

The bubble wall is assumed to be at the saturation temperature corresponding to the ambient pressure:

$$t > 0, \qquad y = 0: \qquad T = T_s \tag{65}$$

The heat balance at the bubble wall, Eq. (14), may be written

$$y = 0: \qquad \frac{\partial T}{\partial y} = \frac{T_{b0} - T_s}{\alpha N_J}\dot{R} \tag{66}$$

New independent variables are now introduced into Eq. (63): $s = y/R$ as a position variable, and $R(t)$ as a time variable, giving

$$\frac{\alpha}{R\dot{R}}\frac{\partial^2 T}{\partial s^2} + \frac{\partial T}{\partial s}\left[1 + s - \frac{1}{(1 + s)^2}\right] = R\frac{\partial T}{\partial R} \tag{67}$$

For uniform temperature fields, $R\dot{R}$ is nearly constant, in which case the variables become separable. A perturbation solution is, therefore, attempted of the form

$$R\dot{R} = b_0 + b_1 R + b_2 R^2 + \cdots \tag{68}$$

$$T - T_s = d_0(s) + b_1 R d_1(s) + b_2 R^2 d_2(s) + \cdots \tag{69}$$

which, on substitution into Eq. (67) and noting that

$$1 + s - (1 + s)^{-2} \cong 3s \tag{70}$$

if $s \ll 1$, gives eventually a set of confluent hypergeometric equations for the temperature field close to the bubble wall. In order to make the equations consistent with the assumed form of the initial temperature distribution, Eq. (64), it is necessary to consider both "inner" and "outer" boundary layer solutions, which are patched together at a convenient intermediate point. For details the reader is referred to the original reference. A comparison is made (Fig. 5) with the numerical solution of Griffith (G7) for the growth of a hemi-

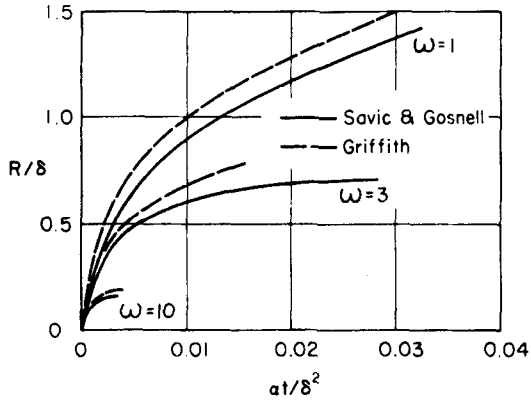


FIG. 5. Bubble growth curves for various $\omega$ (S2).

spherical bubble on a heated plane surface, where the initial temperature decreases linearly through a wall boundary layer, outside of which it is uniform. In order to make a comparison, the inverse thickness of the superheated layer over the surface of the bubble is averaged to give an equivalent spherically symmetric problem In general, the solutions are in agreement within 10 percent. The averaging procedure is justified by an extension of the analysis to axisymmetric temperature distributions. It is also verified, in agreement with Griffith's calculations (G7), by computation of the isotherms when the bubble projects a considerable distance beyond the heating surface boundary layer, that simultaneous vaporization near the bubble base and condensation at the crown occur, as postulated by Ellion (E2). Other arguments for the importance of this latent heat transport mechanism, especially in subcooled boiling, have been presented (B6, B9).

*b. Skinner and Bankoff (S12).* Bankoff and Mikesell (B10) employed, as noted, a variant of the Plesset–Zwick perturbation technique to obtain

bubble growth curves for initial temperatures which were exponential and ramp functions of the Lagrangian radial coordinate $m$. More recently, Skinner and Bankoff (S12) solved the problem for a spherically symmetric, but otherwise arbitrary, initial temperature distribution in the liquid, $f(m)$, and explored some features of the solution.

We define a dimensionless temperature by

$$g(m) \equiv [f(m) - T_s]/[f(0) - T_s] \tag{71}$$

and a dimensionless time by

$$\zeta_1 = \frac{\alpha}{l^2}\int_0^t \mathscr{R}^4(\tau)\, d\tau, \qquad \mathscr{R} = \frac{R}{l} \tag{72}$$

where $l$ is a characteristic length to be chosen later, and $m$ is the position variable defined by Eq. (25). Frequently $f(0) = T_{b0}$, the initial bubble wall temperature, is identified, in the absence of other information, with the heater wall temperature $T_w$. The zero-order solution turns out, for zero initial radius, to be simply

$$\mathscr{R}_0{}^3(\zeta_1) = 3N_J \int_0^\infty g(m)\, \operatorname{erfc}\left(\frac{m}{2\zeta_1{}^{1/2}}\right) dm \tag{73}$$

This result, combined with the inverse of Eq. (72),

$$\frac{\alpha t}{l^2} = \int_0^\zeta \frac{d\zeta'}{\mathscr{R}_0{}^4(\zeta')} \tag{74}$$

gives a parametric representation for the bubble curve.

An important conclusion to be drawn from the form of Eq. (73) is that the nature of the initial temperature distribution some distance away from the bubble wall is of little consequence, so that no restriction need be made that the initial temperature variation occur entirely within a thin thermal boundary layer. For uniform initial superheat the effect of nonzero initial radius is next examined. Taking $l = R(0)$, a simple modification of the analysis leads to

$$\mathscr{R}_0{}^3(\zeta_1) = 1 + N_J(\zeta_1/\pi)^{1/2} \tag{75}$$

Substituting into Eq. (72), one obtains a cubic equation, whose solution is

$$R_0(t) = 2\left(R^2(0) + \frac{4N_J{}^2\alpha t}{\pi}\right)^{1/2} \cos\left[\frac{\pi}{6} + \frac{1}{3}\sin^{-1}\left(1 + \frac{4N_J{}^2\alpha t}{\pi R^2(0)}\right)^{-3/2}\right] \tag{76}$$

This reduces to the leading term of the Plesset–Zwick asymptotic solution, Eq. (43), for large time, or for $R(0)=0$. The displacement between the two bubble radius expressions when the bubble radius has increased tenfold is

less than 2% of the bubble radius. The neglect of the initial radius in the self-similar solutions of Birkhoff *et al.* and Scriven is, therefore, justified, although it should be noted that the effect of neglecting the inertial and surface tension terms has not been considered.

The essential information concerning the behavior of the integral in Eq. (73) can be obtained from an examination of the solution for the initial temperature function $g(m) = 1 - 2am/\pi^{1/2}$, which may be looked upon as a truncated Maclaurin expansion of the temperature field. The first perturbation in the bubble volume was calculated exactly:

$$\frac{V_1}{V_0} = \frac{R_1^3}{R_0^3} = \frac{\frac{4}{9} - \frac{2}{3}\sum_{n=1}^{\infty} \frac{n+6}{(n+1)(n+3)} B\left(\frac{1}{2}, \frac{n}{2}\right) a^n \zeta_1^{n/2}}{N_J(1 - a(\zeta_1)^{1/2})} \tag{77}$$

where $B(p, q)$ is the Beta function. For the uniform superheat case $a = 0$, and Eq. (51) is obtained; at the maximum radius it turns out, for $a > 0$, that

$$\frac{V_1}{V_0} \doteq -\frac{1.7}{N_J}; \qquad \zeta_1 = \frac{1}{4a^2} \tag{78}$$

and when the bubble has collapsed to three-quarters its maximum size,

$$\frac{V_1}{V_0} \doteq -\frac{7.5}{N_J}; \qquad \zeta_1 = \frac{9}{16a^2} \tag{79}$$

Clearly, as time proceeds, this ratio continues to grow, so that the region of applicability of the zero-order solution, based on the thin thermal boundary layer concept, cannot be extended very far into the collapse phase. This is in accord with the physical facts, since the thermal boundary layer thickness is monotonically increasing, while the bubble radius is shrinking.

Computations were carried out in detail for an exponential initial temperature distribution:

$$T(r, 0) = T_\infty + (T_w - T_\infty) \exp(-r^6/9l^6) \tag{80}$$

where $l$ may be thought of as an initial thermal boundary layer thickness, and $l/R \ll 1$ during most of the bubble life. In this case the bubble growing on a heated surface may tend to deform rather than pierce the thermal boundary in which it originates, implying that the temperature gradient near the bubble wall will be normal to it. On substituting into Eqs. (73) and (74), dimensionless radius-time curves were determined for various values of $\omega \equiv (T_w - T_\infty)/(T_w - T_s)$ (Figs. 6 and 7).

Finally, the restriction of spherically symmetric initial distributions can be removed, so that the solution for general initial temperature fields of the

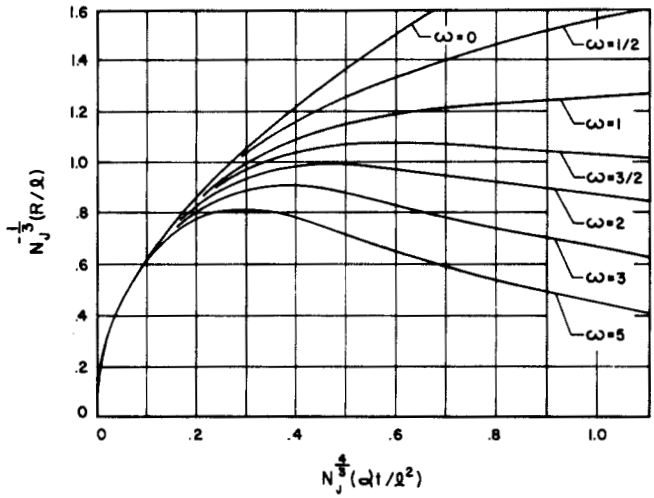


FIG. 6. Bubble growth curves for various $\omega$ (S12); $\omega > 1$ corresponds to subcooled boiling, $\omega = 1$ to saturated boiling, and $\omega = 0$ is the uniform initial superheat case.

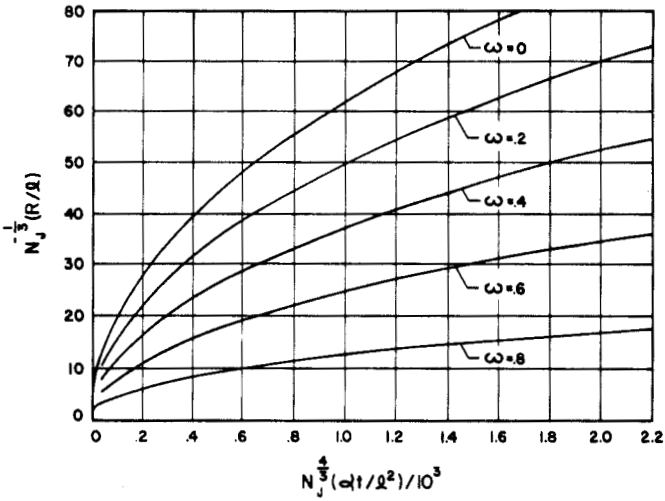


FIG. 7. Bubble growth curves for cases when the bulk liquid is superheated, $0 \leqslant \omega < 1$ (S12).

form $T(r, \theta, \varphi, 0) = f(r, \theta, \varphi)$ can be found (S11). For this problem the Laplacian operator on the right-hand side of Eq. (22) is given by

$$\nabla^2 = \frac{1}{r^2}\frac{\partial}{\partial r}\left(r^2\frac{\partial}{\partial r}\right) + \frac{1}{r^2}\sin\theta\frac{\partial}{\partial\theta}\left(\sin\theta\frac{\partial}{\partial\theta}\right) + \frac{1}{r^2}\sin^2\theta\frac{\partial^2}{\partial\varphi^2}$$

while the energy balance at the bubble wall now requires

$$\frac{dR}{dt} = \frac{k}{4\pi L\rho'} \int_0^{2\pi} \int_0^{\pi} \frac{\partial T(R, \theta, \varphi, t)}{\partial r} \sin\theta \, d\theta \, d\varphi \tag{81}$$

assuming constant vapor density and latent heat in the asymptotic bubble growth phase. With the introduction of the averaged temperature excess

$$\Theta(r, t) = \frac{1}{\Delta T} \int_0^{2\pi} \int_0^{\pi} [T(r, \theta, \varphi, t) - T_s] \sin\theta \, d\theta \, d\varphi \tag{82}$$

where

$$\Delta T = \int_0^{2\pi} \int_0^{\pi} [f(0, \theta, \varphi) - T_s] \sin\theta \, d\theta \, d\varphi \tag{83}$$

the differential equation, with associated initial and boundary conditions, then becomes

$$\frac{\partial\Theta}{\partial t} + \frac{dR^3/dt}{3r^2} \frac{\partial\Theta}{\partial r} = \frac{\alpha}{r^2} \frac{\partial}{\partial r}\left(r^2 \frac{\partial\Theta}{\partial r}\right) \tag{84}$$

$$\Theta(r, 0) = \frac{1}{\Delta T} \int_0^{2\pi} \int_0^{\pi} [f(r, \theta, \varphi) - T_s] \sin\theta \, d\theta \, d\varphi \triangleq g(r) \tag{85}$$

$$\frac{dR}{dt} = \alpha N_J'' \frac{\partial\Theta(R, t)}{\partial r} \tag{86}$$

$$\Theta(R, t) = 0 \tag{87}$$

The constant $N_J''$ in Eq. (86) is a generalized Jakob number defined by

$$N_J'' = k\,\Delta T/\rho' L\alpha \tag{88}$$

In this form the parametric solutions, Eqs. (73) and (74), for the spherically symmetric problem can be applied immediately. Physically this implies that a bubble growing in an initially arbitrary temperature field grows at precisely the same rate as if the initial temperature were averaged in each thin spherical shell surrounding the bubble center. Two special cases are considered in detail: (*1*) the linear thermal boundary layer, of thickness $l$, next to the heating surface, outside of which the temperature is uniform; and (*2*) the exponential boundary layer, where the temperature is assumed to decay exponentially with distance from the wall. The latter distribution is of the form

$$f(r, \theta) = T_\infty + (T_w - T_\infty) \exp\left(-\frac{2r\cos\theta}{l}\right), \qquad 0 < \theta \leqslant \pi/2 \tag{89}$$

It should be noted that in attempting to connect the temperature distributions given by Eqs. (80) and (89) to surface boiling, two separate limiting cases are being considered. Equation (80) implies that the thermal boundary layer associated with the hot surface becomes deformed around the bubble in a manner leading to the approximation of an initially spherically symmetric temperature distribution. This picture seems reasonable when the bubble radius at the start of asymptotic growth is somewhat larger than the thermal boundary layer thickness. On the other hand, Eq. (89) implies that the boundary layer thickness is large compared with the initial radius, so that the temperature field is essentially undisturbed as the bubble enters the asymptotic stage. The further assumptions are made that the bubble is hemispherical, thermal coupling between the vapor phase and the boiling surface is poor, and liquid heating across the surface is sufficiently low to be negligible over the bubble lifetime. Under these assumptions one has the equivalent problem of an entire vapor sphere growing in a liquid whose temperature field is symmetric about the equator plane.

The explicit solution for the exponential thermal boundary, Eq. (89), is conveniently expressed in parametric form

$$R^3(z) = \frac{6N_J''z^3}{(\pi)^{1/2}}[1 - \omega\psi(z)] \tag{90}$$

$$\tau = \frac{\alpha t}{l^2} = \left(\frac{\pi^2}{6N_J''^4}\right)^{1/3} \int_0^z \frac{z\,dz}{[1 - \omega\psi(z)]^{4/3}} \tag{91}$$

where

$$\psi(z) = 3\sum_{n=1}^{\infty} \frac{(-1)^{n+1}\Gamma(n/6 + 1)}{(n + 3)(n + 1)!}(48z^3)^{n/3} \tag{92}$$

These solutions are shown in Fig. 8, where $\omega = 0$ represents uniform initial superheat. As the subcooling of the bulk liquid increases, a relatively long period of very slow change in radius is predicted. Similar behavior is frequently noted in boiling from surfaces.

For the linear case,

$$f(r, \theta) = \begin{cases} T_\infty, & 0 < \theta < \cos^{-1} l/r \\ T_\infty + (T_w - T_\infty)\dfrac{r\cos\theta}{l}, & \cos^{-1} l/r < \theta < \pi/2 \end{cases}, \quad r/l > 1$$
$$T_\infty + (T_w - T_\infty)\left(1 - \frac{r\cos\theta}{l}\right), \quad r/l < 1 \tag{93}$$

The solution is somewhat more complicated (and is hence not given here), but leads to slightly larger bubble volumes (Fig. 9) than the exponential

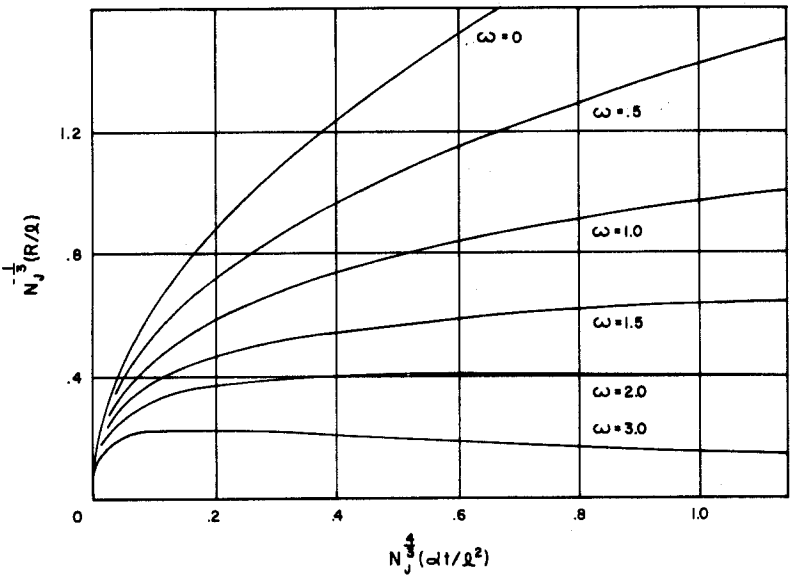


FIG. 8. Bubble growth curves for various $\omega$ for the case of exponential thermal boundary (S11).

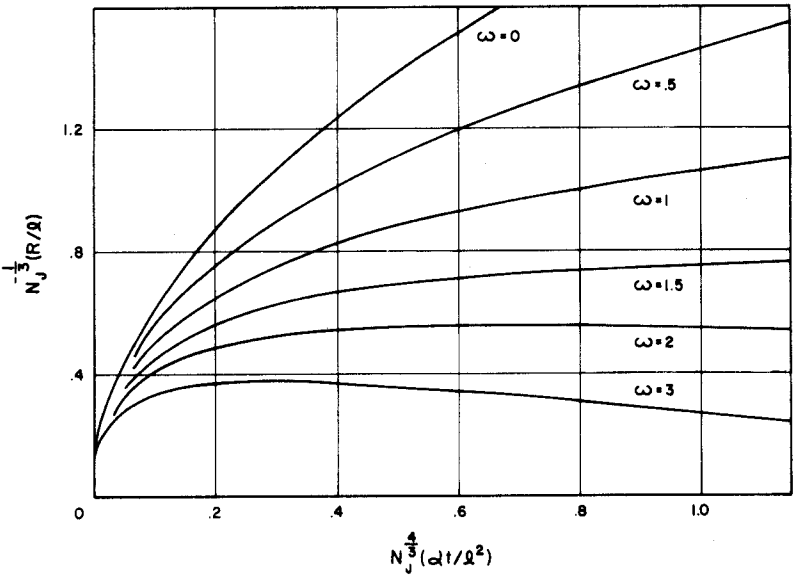


FIG. 9. Bubble growth curves for various $\omega$ for the case of linear thermal boundary (S11).

boundary of equivalent superheat energy. This is to be expected, in view of the slightly greater thickness of the equivalent exponential layer. A comparison is made of the linear boundary solution at $N_J = 5.3$ with Griffith's numerical solution of a similar problem (G7), in which the initial condition is given by Eq. (93), but a boundary condition is imposed of the form $T = T_w$ at $\theta = \pi/2$. Griffith's growth rates are somewhat larger, since the wall now continues to transfer heat into the system after bubble growth has commenced (Fig. 10).

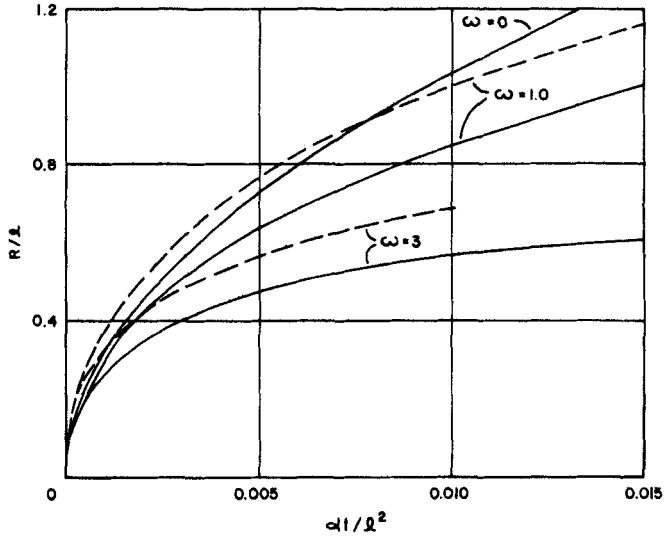


FIG. 10. Comparison between linear boundary solution and Griffith's numerical solution (dashed lines) at $N_J = 5.3$ (S11).

*c. Dougherty and Rubin (D6).* Dougherty and Rubin consider the growth and collapse of vapor bubbles on a boiling surface by expanding the temperature field in terms of spherical harmonics, and retaining only the zero-order term. This is equivalent to averaging the temperature in the tangential direction. Although inertial terms are dropped, the small variation in vapor superheat with time, as well as the surface tension and viscous terms, are retained in arriving at a nonlinear integral equation for the radius of the vapor bubble. In the asymptotic stages this reduces to

$$R^2(t) \simeq R_1^2(t) + \int_{t_0}^{t} \{K(t-\tau)^{1/2}[R_i - (R - R_0)] - (t-\tau)\dot{R}^2(\tau)\}\, d\tau$$
$$K = \frac{4L^2\rho'}{k\varepsilon T_s}\left(\frac{\rho'}{\rho}\right)\left(\frac{\alpha}{\pi}\right)^{1/2} \tag{94}$$

where $R_i$ is the radius of an isothermal vapor bubble whose vapor phase

remained at saturation temperature and pressure throughout the growth and collapse stages, and $t_0$ is the time at which asymptotic growth commences. $R_1$ is the bubble radius at the commencement of asymptotic growth and is given by a separate integral equation. At this point an argument is employed from the calculus of variations. Noting that the left-hand side of Eq. (94) is positive semidefinite, the collapse time is argued to correspond to a stationary point of the functional on the right-hand side. This is incorrectly stated to lead to a linear Euler equation for $R(t)$,

$$t\ddot{R} + \dot{R} - \tfrac{1}{2}K(t)^{1/2} = 0 \tag{95}$$

whereas the correct Euler equation[7] is

$$(t_c - t)\ddot{R}(t) + \dot{R}(t) - \tfrac{1}{2}K(t_c - t)^{1/2} = 0 \tag{96}$$

Upon application of the boundary condition $R(t_c) = 0$ the solution to this equation blows up.

*d. Han and Griffith (H2).* For the growth of a single bubble in a liquid of initially uniform superheat, all theories (including the simple plane approximation) predict that the radius asymptotically grows as the square root of time. Furthermore, the range of the predicted growth constants is relatively small. Noting this, Han and Griffith employ an empirical correction factor to take into account curvature and stretching of the thermal boundary layer, using the plane approximation. In addition, an empirical heat transfer coefficient, chosen to give best agreement with data, is defined for the heat transfer between the wall and the bubble base. The calculation is now very simple. A linear temperature profile is assumed initially in some thermal boundary layer next to the wall and a constant temperature outside of this region. A simplified model of bubble growth is taken, shown in Fig. 11, leading to the following equation for bubble growth:

$$\frac{dR}{dt} = \frac{\varphi_c \varphi_s}{\varphi_v} \frac{k}{\rho' L} \frac{\partial T(0, t)}{\partial x} + \frac{\varphi_b \tilde{h}(T_w - T_s)}{\varphi_v \rho' L} \tag{97}$$

where $\varphi_c$ is the curvature factor to be discussed below; $\varphi_s = (1 + \cos \varphi)/2$ is a surface factor which represents the ratio of the surface of the spherical segment to that of the complete sphere, and $\varphi_b = (\sin^2 \varphi)/4$ and $\varphi_v = [2 + \cos \varphi(2 + \sin^2 \varphi)]/4$ are similar base and volume ratios. Here $\varphi$ is the contact angle, while $\tilde{h}$ is the heat transfer coefficient from heating surface to steam bubble through its base area. It is important to note the assumption that the thermal boundary layer around the bubble is the same as that next to the wall. This implies physically that the bubble picks up the thermal boundary layer as it grows from a relatively small size, which is a plausible

[7] This was pointed out by Professor L. A. Skinner (S13b).

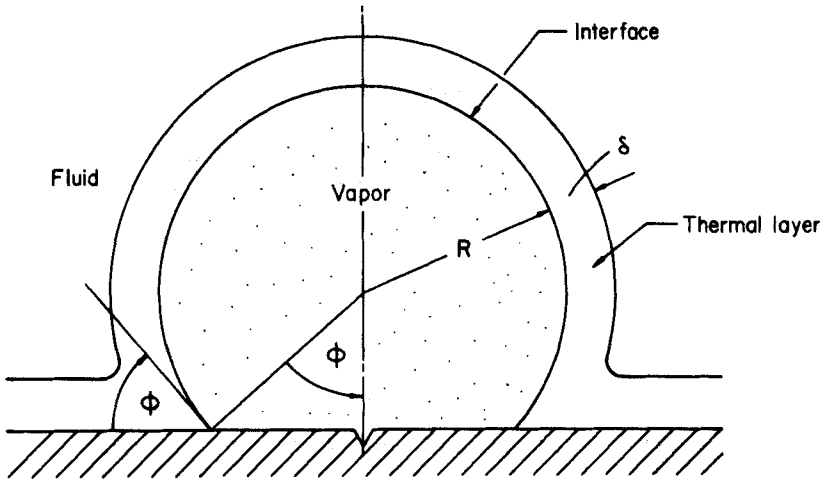


FIG. 11. Simplified model of bubble growth (H2).

limiting case for $N_J \gg 1$. However, one would expect, in this case, the boundary layer stretching error to be appreciable. On substituting the semi-infinite slab solution for the heat flux at the bubble wall one obtains

$$\frac{dR}{dt} = \frac{\varphi_c \varphi_s}{\varphi_v} \frac{k}{\rho' L} \frac{1}{(\pi\alpha t)^{1/2}} \left[ T_w - T_s - \frac{(T_w - T_\infty)}{\delta} (\pi\alpha t)^{1/2} \operatorname{erf}\left( \frac{\delta}{(4\alpha t)^{1/2}} \right) \right] + \frac{\varphi_b \tilde{h} (T_w - T_s)}{\varphi_v \rho' L} \tag{98}$$

where $\delta = (\pi\alpha t_w)^{1/2}$ is the computed thermal boundary layer thickness, and $t_w$ is the waiting period between bubbles. For a bubble growing in an infinite fluid of uniform superheat this reduces to

$$\frac{dR}{dt} = \frac{\varphi_c k}{\rho' L} \frac{(T_w - T_s)}{(\pi\alpha t)^{1/2}} = \frac{\varphi_c}{\pi^{1/2}} N_J \left( \frac{\alpha}{t} \right)^{1/2} \tag{99}$$

For the exact solution, Eq. (20), for a uniform initial superheat, $\varphi_c = \sqrt{3}$, while the plane approximation, treating the liquid surrounding the bubble as a semi-infinite slab, gives $\varphi_c = 1$. It is incorrectly stated then that, for $\varphi = 0$ and $\delta \ll R$, the Plesset–Zwick thin thermal boundary layer solution leads to $\varphi_c = \pi/2$, whereas, as noted above, it agrees asymptotically with the exact solution. An empirical curvature factor is then manufactured to account for all three assumed cases,

$$\varphi_c = \left[ \sqrt{3} + \frac{\varphi}{\pi}(1 - \sqrt{3}) \right] \left[ \left( 1 - \frac{\varphi}{\pi} \right) \frac{[(\pi/(2\sqrt{3}))\bar{R} + \delta]}{\bar{R} + \delta} + \frac{\varphi}{\pi} \right] \tag{100}$$

where $\bar{R}$ is the time-average bubble radius. Fairly good agreement is shown

with the measured $R(t)$ of only three bubbles growing in distilled water at atmospheric pressure. It is evident that this theory, which may be useful for rough calculations, requires considerable additional experimental verification.

## D. Two-Component Liquids

Van Wijk (V1) and Van Wijk, Vos, and Van Stralen (V3) pointed out that the temperature difference between a superheated binary liquid mixture and the dew point of the vapor bubbles which are formed shows a minimum at a certain low concentration of the more volatile component, and suggested that the bubble growth rate would also be least at this point. In the case of methyl ethyl ketone–water mixtures the minimum occurred at 4.1 wt. % ketone, which coincided with the experimentally observed maximum heat flux.

Scriven (S3), however, was the first to show that a self-similar solution could be found for a binary mixture of uniform initial temperature and composition. Detailed calculations were presented for the ethylene glycol–water system, shown in Fig. 12. In line with the observations of Van Wijk *et al.*, it

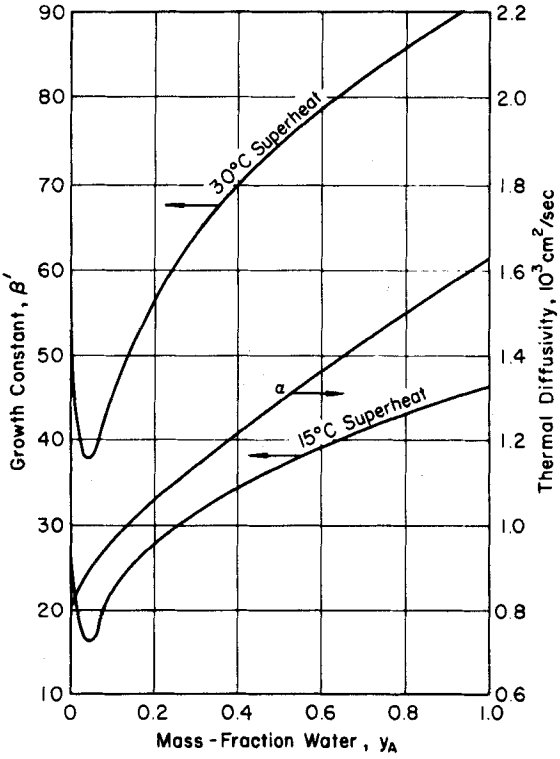


FIG. 12. Bubble growth in water–ethylene glycol solutions at 1 atm (S3).

is shown that the growth constant $\beta$ goes through a minimum at about 0.05 wt fraction of water. This is attributable to the depletion of the volatile component near the bubble wall, while at the same time the temperature has been sufficiently depressed so that the volatility of the glycol is relatively low.

A more general two-component bubble growth solution (S13) permits both the initial temperature and concentration to be arbitrary functions of the radial distance. The same procedures used to solve the single-component problem are employed. A general solution is obtained and various limiting cases examined. For uniform initial conditions the solution is in agreement with the exact solution under conditions which assure rapid convergence of the perturbation procedure. An example problem is worked out for exponential temperature and concentration boundary layers initially surrounding the bubble. The process is somewhat more complicated than in single-component calculations since the time-average bubble temperature is not known *a priori*, so that an iterative scheme has to be established. By the space-averaging procedure discussed above it is thought that this technique can be extended to arbitrary initial temperature and concentration fields, so that this problem may be considered to be, in principle, solved.

## E. Gas Bubble Growth

For isothermal gas bubble growth at atmospheric pressure, $N_J'$ is usually small (Section II,B,1), so that $\beta_3 \cong (2N_J')^{1/2}$. This result is identical with that obtained by computing the concentration distribution at any instant from the Laplace equation (quasi-steady state approximation), and determining the bubble growth rate from the computed concentration gradient at the bubble wall. Kirkaldy (K4) discusses the conditions under which this simplification can be considered; a necessary condition is that the diffusion boundary layer thickness increase rapidly compared to the bubble radius, which is implied by small $\beta$. A less drastic simplification entails the neglect of the convective term, but not the time derivative, in the diffusion equation (quasi-stationary assumption). Fricke (F8) and Epstein and Plesset (E3) apply this approximation to the growth or dissolution of gas bubbles, and arrive at the result

$$\frac{dR}{dt} = \mathscr{D}N_J'\left[\frac{1}{R} + \frac{1}{\delta}\right], \qquad \delta = (\pi\mathscr{D}t)^{1/2} \tag{101}$$

This equation is solved exactly by Epstein and Plesset, and is also extended to include surface tension effects. Generally, for gas bubble growth, $\delta/R \gg 1$, corresponding to $\beta \ll 1$, and Eq. (101) reduces to the quasi-steady solution. This is in agreement with the limiting result obtained from the exact solution $R \propto (2N_J'\mathscr{D}t)^{1/2}$. On the other hand, when a gas bubble begins to dissolve,

$\delta/R \ll 1$; it is seen from Eq. (101) that, for this limiting case also, $R \propto t^{-1/2}$. However, eventually $\delta/R \gg 1$ for a dissolving bubble, so that the steady-state solution prevails. For gas bubbles dissolving in water at atmospheric pressure with $R(0) < 0.2$ mm, Houghton, Ritchie, and Thomson (H8) find that the transient term becomes negligible after about 100 sec. After this time the result reduces to the quasi-steady solution, governed by the Laplace equation, whose solutions have been extensively studied. For a bubble attached to a wall with zero contact angle, Liebermann (L6) thus shows that the rate of solution is reduced by a factor of ln 2, leading to the result

$$R^2(t) = R^2(0) - \frac{2\mathscr{D}N_J't}{\ln 2} \tag{102}$$

Manley (M3) extends this result to allow for nonzero contact angle.

Bruijn (B24) employs the quasi-stationary approximation, as discussed in Bankoff (B8), to the growth of vapor bubbles in superheated binary liquid mixtures. As noted previously, this neglect of the convective term in the diffusion equation is justified only when $N_J \ll 1$, which is usually not the case in atmospheric boiling. On the other hand, this technique would be applicable to isothermal gas bubble growth in three-component systems, where two of the components are dissolved gases.

Flatt (F3) computes bubble growth rates due to radiolytic gas formation in a power excursion in a homogeneous reactor. For very small bubbles the growth is assumed to be quasi-stationary so that the convective term can be dropped from the diffusion equation. A distributed exponential volume source is assumed. An integral equation for the radius is then obtained, from which upper and lower bounds for the radius of the bubble can be deduced.

For isothermal gas bubble growth in liquids of arbitrary initial concentration distribution, where the boundary layer volume is large compared to the bubble volume, it is recommended (S12) that a straightforward modification of the Epstein and Plesset (E3) quasi-stationary technique be employed.

## III. Experimental Bubble Growth Data

### A. Vapor Bubbles

A classical set of experiments was performed by Dergarabedian (D2, D3) who irradiated water, carbon tetrachloride and other liquids, and photographed the asymptotic growth of minute bubbles originating within this uniformly superheated liquid. The superheat range was 2 to 10°C, and the pressure atmospheric, corresponding to $N_J > 1$. The initial and boundary conditions corresponded to the theory, so that the results are susceptible of

relatively unequivocal interpretation. As might be expected, the Plesset–Zwick theory gives good agreement with these results. The Forster–Zuber expression, Eq. (60), also gives good agreement with these data, despite the fact that the growth constant differs by 9%. This arises from the arbitrary choice of zero time for the asymptotic stage. For a more exact comparison of theory with experiment, microscopic bubble growth data would also have to be available. In most industrially important applications, however, bubbles grow while attached to solid surfaces, and most bubble growth data have been similarly obtained. Measurements of bubble growth in saturated or slightly subcooled pool boiling have been made by Patten (P1) of water at subatmospheric pressures from wires, and at atmospheric pressure by Vos and Van Stralen (V5) and Van Wijk and Van Stralen (V2) of water and water–methyl ethyl ketone mixtures from wires; by Bankoff and Mikesell (B11), based upon motion pictures taken by Zmola (Z3), of water from a horizontal strip; by Strenge, Orell, and Westwater (S16) of pentane and ether from a flat vertical surface; and by Benjamin and Westwater (B17, B18) of water–ethylene glycol mixtures from a vertical copper surface with an artificial nucleation site. None of these experiments permits direct confirmation of the exact or of the boundary layer theories. The presence of the solid wall or wire, to an unknown degree, results in a distortion of the purely radial flow pattern postulated by the theory. More important, no measurements are available of the temperature (and/or concentration) fields in the liquid surrounding a bubble entering the asymptotic stage of growth. Without this information a discussion of the significance of the data and comparison with theory is necessarily of a heuristic nature. Nevertheless, some general observations can be made concerning all the data on saturated pool boiling:

*1.* Bubble growth from flat surfaces is almost always statistical in nature. This is apparently due to liquid turbulence induced by the wake of departing bubbles, coalescence with neighboring bubbles, momentary oscillating pressure fields within the fluid, and possible statistical variations in the nucleating surface. An exception is found in the experiments of Benjamin and Westwater (B17), who employed a 0.004-in. artificial cavity from which it was possible to produce a single stream of isolated bubbles. To some extent the same statistical behavior is observed in boiling from wires, although a greater degree of regularity seems to be present. For both horizontal surfaces and wires some bubbles were observed to vibrate, both before and after breaking away from the heating surface.

*2.* Even when photographed at framing speeds in excess of 5000 frames/sec, much of the total increment in bubble radius occurs in the first few frames. After this initial rapid growth period, $t^{-1/2}R(t)$ usually decreases with time. The bubble is thus growing during most of its observable lifetime on the heating surface more slowly than predicted by the uniform superheat theory.

Perhaps the most extensive investigation is that of Strenge, Orell, and Westwater (S16), who plotted $R(t)$ on log-log paper for 86 pentane bubbles originating from a zinc surface with a superheat of 12°F. Upon fitting the best straight line to the late asymptotic data, a considerable statistical variation was observed, the mean exponent being 0.40, with a standard deviation of 0.04. A number of similar measurements were made at various heat fluxes and also in ether. Similar results were reported by Benjamin and Westwater for glycol–water mixtures. Although Scriven's theory is thus not applicable to these data, a qualitative confirmation was found of the theoretical prediction that the minimum growth coefficient occurs at about 5 wt-% in water–ethylene glycol mixtures.

Darby (D1) has recently made a photographic study of boiling of water and Freon 113 from a single nucleation site induced by external infrared irradiation. Surprisingly enough, the bubble radius was found to vary closely as $t^{2/3}$ both before and after breakoff for all recorded runs. The data for both liquids were correlated by an expression of the form

$$R = 1.04A_1^{2/3}(g\sigma)^{1/12}\left(\frac{c_p k}{L^2}\right)^{1/3}\left(\frac{\rho}{\rho'}\right)^{5/12}(T - T_s)^{2/3}t^{2/3} \tag{103}$$

where $A_1$ is a constant obtained by comparison with the experimental data. It is not clear why the time exponent is so high, especially since the equipment is quite similar to that employed by Dergarabedian. One possibility is that the thermal boundary layer surrounding the bubble received an appreciable amount of irradiation after the initiation of growth, suggested by the fact that a continuous stream of bubbles was induced.

### B. Gas Bubbles

Isothermal gas bubble growth, on the other hand, can be expected to conform more closely to the assumption of uniform initial conditions, since here the diffusion boundary layer is relatively thick. Westerheide and Westwater (W2, W3) measured the growth of hydrogen bubbles on a platinum cathode at constant emf (Fig. 13). The theoretical curves are obtained by calculating the growth constants in the exact solution which gives best fit with data. In the late asymptotic stage the faster-growing bubbles deviate significantly from this theoretical curve, presumably because the boundary layer thickness on the cathode is comparable to that of the bubble. It is found that the quasi-stationary solution, Eq. (101), gives a growth rate which is low by a factor of 14–21% when the theoretical supersaturation obtained by the above curve fitting is substituted. This is to be expected in view of the high modified Jakob numbers ($N_J' \sim 0.4$), so that the quasi-stationary assumption would not be appropriate for such large supersaturations.

More extensive measurements of the growth of electrolytic bubbles were obtained by Glas and Westwater (G3), who made a number of interesting observations which will be reviewed here in some detail. The electrodes used

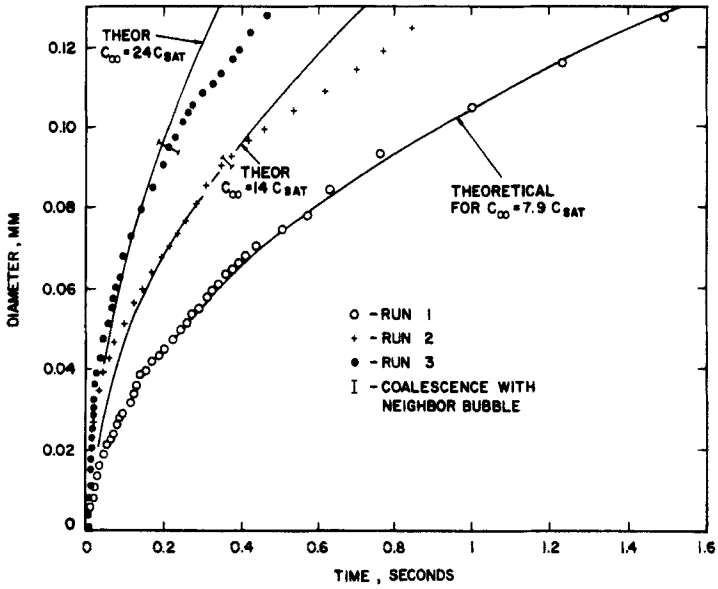


FIG. 13. Growth of hydrogen bubbles during electrolysis at constant emf. Run 1: 1$N$ $H_2SO_4$, 1.24 v; Run 2: 0.1$N$ $H_2SO_4$, 1.23 v; Run 3: 0.1$N$ $H_2SO_4$, 1.47 v (W2).

were 0.127–0.508-mm wires of Pt, Ni, Fe, and Cu; the electrolytic gases were $H_2$, $O_2$, $Cl_2$, and $CO_2$. Most bubbles (Fig. 14) exhibited excellent straight-line plots of $D$ vs $t^{1/2}$, from whose slope the effective supersaturation pressure can be calculated, based upon the self-similar solution for uniform initial conditions given by Birkhoff *et al.* (B19), and by Scriven (S3). Figure 15 shows a plot of the dimensionless driving force, $N_J'/(1 - C_s/\rho) \equiv \Phi$, vs the growth coefficient, $\beta = 2\beta'$, where $\beta'$ is the growth coefficient defined by Scriven. It is seen that, except near the critical pressure, $\Phi$ is very nearly equal to $N_J'$. In the same figure is shown the curve numerically computed by Buehl and Westwater (B25) for a bubble growing tangent to a wall which is not acting as a source of dissolved gas. At all $N_J'$ the effect of the wall is to reduce the growth rate, but at $N_J' \sim 1$, the effect becomes negligible. On the other hand, for very slow growth $\beta$ is about 30 percent smaller than in the absence at the wall.[8] The supersaturation ratios $C_\infty/C_s$ computed in this

[8] As $N_J' \to 0$, corresponding to quasi-steady motion, the growth coefficient should be reduced by a factor of ln 2, as in Eq. (102), in agreement with the numerical solution.

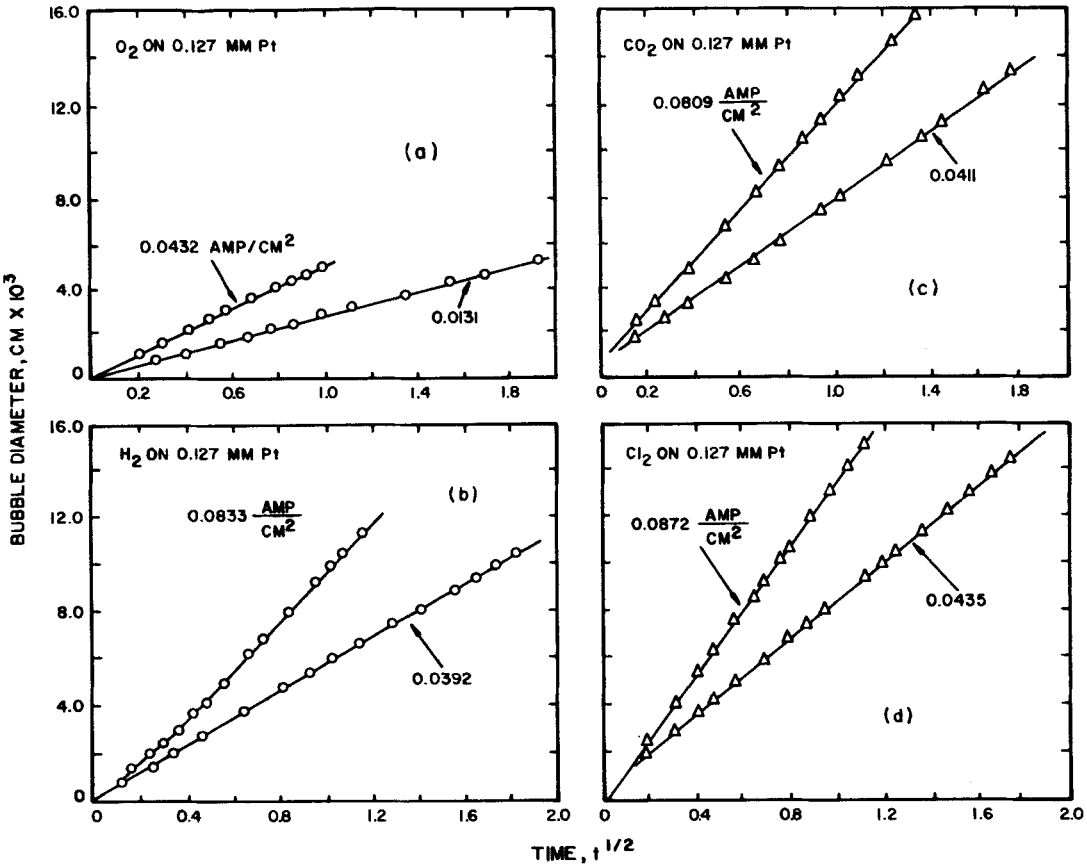


FIG. 14. Typical growth data for 8 bubbles at 1 atm: (a) $O_2$ in 1.0*N* $H_2SO_4$, (b) $H_2$ in 1.0*N* $H_2SO_4$, (c) $CO_2$ in 1.0*N* $Na_2C_2O_4$ plus 30% $H_2SO_4$, (d) $Cl_2$ in 1.0*N* NaCl plus 0.01*N* NaOH (G3).

manner were 1.5/19.9 for $H_2$, 1.4/15.4 for $O_2$, 1.1/1.6 for $CO_2$, and 1.02/1.32 for $Cl_2$. Two separate models were proposed to correlate the effect of current density on $\beta$. A "steady-state" model considers the bubble volume (and hence $\beta^3$) at any instant after growth initiates, to be proportional to the current density: $\beta' I^{-1/3} = k_1$, a constant. An "unsteady-state" model, patterned

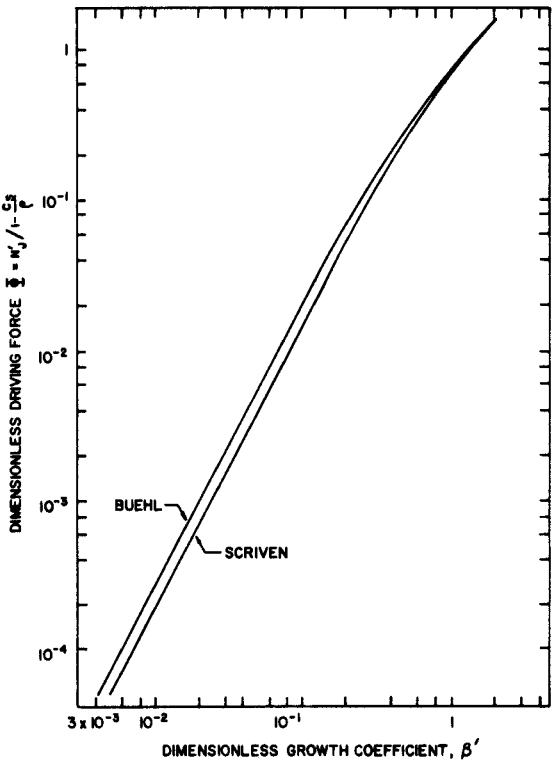


FIG. 15. Theoretical bubble growth constant at 1 atm: Scriven's values are for an isolated sphere; Buehl's values are for a sphere tangent to a plane (G3).

after a model proposed by Hsu (H10) for the analogous heat-transfer problem, computes the boundary layer thickness at the initiation of bubble growth from the observed waiting time $t_w$ between bubbles. From the measured current density the average supersaturation $C_\infty - C_s$ in the boundary layer can be computed. Assuming that the bubble grows in a uniform field of this average supersaturation, the dependence of $\beta'$ on the current density $I$ can be computed (Fig. 16). In this figure, $k_1$ has been chosen for best fit of the data. Typical waiting times were 0.02–0.1 sec, and typical boundary layer thicknesses, $\delta_w \cong (\pi \mathscr{D} t_w)^{1/2}$, were of the order of $1 \times 10^{-3}$ cm. The difficulty in the latter approach now becomes apparent, in that $D/\delta_w > 1$, for nearly all

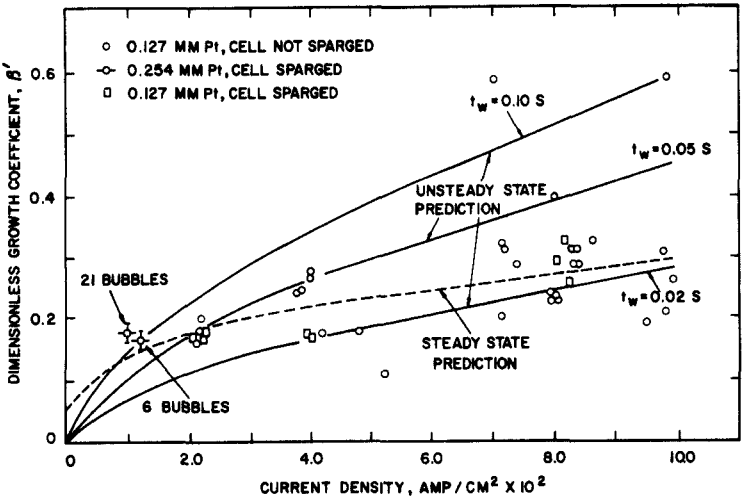


FIG. 16. Illustration of two theoretical models for effect of current density. $H_2$ on Pt in 1.0*N* $H_2SO_4$ at 1 atm (G3).

the data points, so that the assumption that the bubble grows in a uniformly supersaturated fluid does not appear to be physically correct.

Another interesting result reported by Glas and Westwater was that hydrogen bubbles evolving from a polished nickel electrode (Fig. 17) showed an initially very rapid growth period, $< 7 \times 10^{-4}$ sec, followed by a late asymptotic period during which $(t^{1/2}\dot{R})$ was substantially constant. Note that

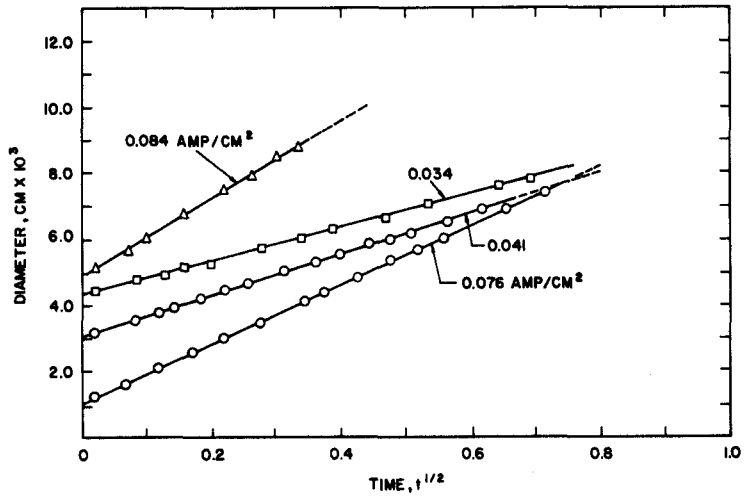


FIG. 17. Very rapid early growth in one movie frame followed by normal growth. $H_2$ on four different sites on 0.127 mm Ni cathode in 1.0*N* $H_2SO_4$ at 1 atm (G3).

here $[R(t) - R(t_0)]$ increases as the square root of time, where $R(t_0)$ is the radius at the start of the late asymptotic growth, which is considerably different from the prediction of the self-similar solution, $R(t) \sim t^{1/2}$. It was observed that $t_w$ was larger for this particular surface, resulting in higher supersaturations, possibly because of a higher degree of polish. All bubbles showed this initially very rapid growth, although usually the total growth in this period was sufficiently small that the extrapolated growth line (Fig. 14) passes close to the origin.[9]

The solution of gas bubbles is, in principle, a valuable means of measuring liquid-phase diffusivities. Mache (M2), Brandstaetter (B23), Liebermann (L6), and Manley (M3) measured the rate of solution of stationary air bubbles in partially saturated water. In general, the rate of diffusion at small bubble diameters is less than expected from theory; the probable explanation seems to be the accumulation of a film of organic material and/or dust particles at the bubble surface. Houghton, Ritchie, and Thomson (H8) extended the method to diffusivity measurements of a number of other gases. Doremus (D5) and Greene and Gaffney (G6) measured the solution rate of oxygen bubbles in molten glass.

## IV. Surface Boiling

### A. Subcooled Boiling

As the bulk temperature of the liquid some distance away from the heating surface is decreased, the characteristics of the bubbles growing at the surface undergo a marked change. The bubbles become smaller and of higher fre-

[9] This behavior cannot be predicted by the self-similar theory. Indeed, it would be difficult to construct a physically reasonable nonuniform initial concentration distribution surrounding an isolated bubble which approximates this behavior. In order to do this, the supersaturation some distance from the bubble wall would be required to be uniform, but positive, while a thin layer of liquid at the bubble wall was initially very much more highly supersaturated. The measurements thus agree with the specific prediction of the uniform supersaturation theory that the bubble wall velocity decreases as the square root of time; but it seems quite likely that this is coincidental. In fact, the observed behavior more nearly coincides with the phenomenological viewpoints advanced by Zuber (Z4), Moore and Mesler (M7), and others (to be discussed briefly later) that the bubble initially grows within a thin, highly supersaturated layer, during which period growth is quite rapid. After its diameter becomes large compared to this layer, its growth slows down, and is controlled by the advance of the bubble wall into a fresh supply of supersaturated liquid. Throughout this process the possibility of gas evolution from a microlayer of liquid at the bubble base may be important. Obviously, these questions can be answered only by further experimental work. Incidentally, Glas and Westwater (G3) note that the contact angle, determined from the bubble radius and height, continuously decreases during bubble growth, assuming that the departure from sphericity was negligible. This decrease in apparent contact angle is not inconsistent with the notion that the advancing bubble leaves behind a thin tongue of liquid at the bubble base.

quency, and eventually cease entirely to detach. Coincidentally, the maximum heat flux which can be sustained at the wall increases. Gunther and Kreith (G10) reported a heat flux as high as 5 Btu/(sq in.)(sec) could be transferred to a pool of distilled water subcooled 145°F below saturation temperature, and Gunther (G9) reported that this limit could be increased by a factor of four by forced convection. Such enormous heat transfer rates have led to applications in cooling of rocket motors and other compact power devices. In a pool of water subcooled more than 100°F the surface boiling activity consists of a random distribution of very small vapor bubbles which never detach from the heating surface, but grow and collapse hemispherically with lifetimes less than one millisecond. In many respects these isolated hemispherical bubbles represent a simpler phenomenon than the loose, irregularly defined bubbles arising in saturated boiling. In Fig. 18 typical $R(t)$ curves are shown for hemispherical bubbles originating on a stainless steel heater strip in distilled water at a temperature of 98°F. The camera framing rate was 14,000 frames per second, made possible by the use of a Kerr electro-optical shutter. It is of interest to note that the growth and collapse portions are nearly mirror images. At small subcoolings the collapse time is several times greater than the growth time. However, as the subcooling is increased, the asymmetry decreases and eventually disappears, for all practical purposes. Another interesting result shown in Fig. 18 is the temperature observed by a thermocouple traverse in the vicinity of the heating surface. In the two-phase region the observed temperature is a weighted average of the vapor and liquid temperatures. The fact that the saturation temperature corresponds to about half the maximum bubble radius away from the wall indicates that the liquid surrounding the top of the bubbles is substantially subcooled.

Symmetrical growth and collapse curves of the sort pictured herein are difficult to obtain by a laminar-flow heat-convection model. This is because the heat equation is not symmetric with respect to time reversal. On the other hand, such symmetry is observed in the growth and collapse of cavitation bubbles, and indeed, is implied by the extended Rayleigh equation (B11):

$$R\frac{d^2R}{dt^2}+\frac{3}{2}\left(\frac{dR}{dt}\right)^2+\frac{2\sigma}{\rho R}=\frac{\Delta p}{\rho}, \qquad \Delta p = p(R)-p_\infty \tag{104}$$

If experimental growth and collapse bubble radius data are employed, this equation can be numerically integrated to obtain $\Delta p$, the difference between the pressure at the bubble wall and in the surroundings, as a function of time (P3). If $\Delta p$ can be assumed to be nearly constant, the first integral of this equation is readily obtained,

$$\left(\frac{dR}{dt}\right)^2 \cong \frac{2\sigma}{\rho}\left[\frac{R_m^2-R^2}{R^3}\right]-\frac{2}{3}\frac{\Delta p}{\rho}\left[\frac{R_m^3-R^3}{R^3}\right] \tag{105}$$

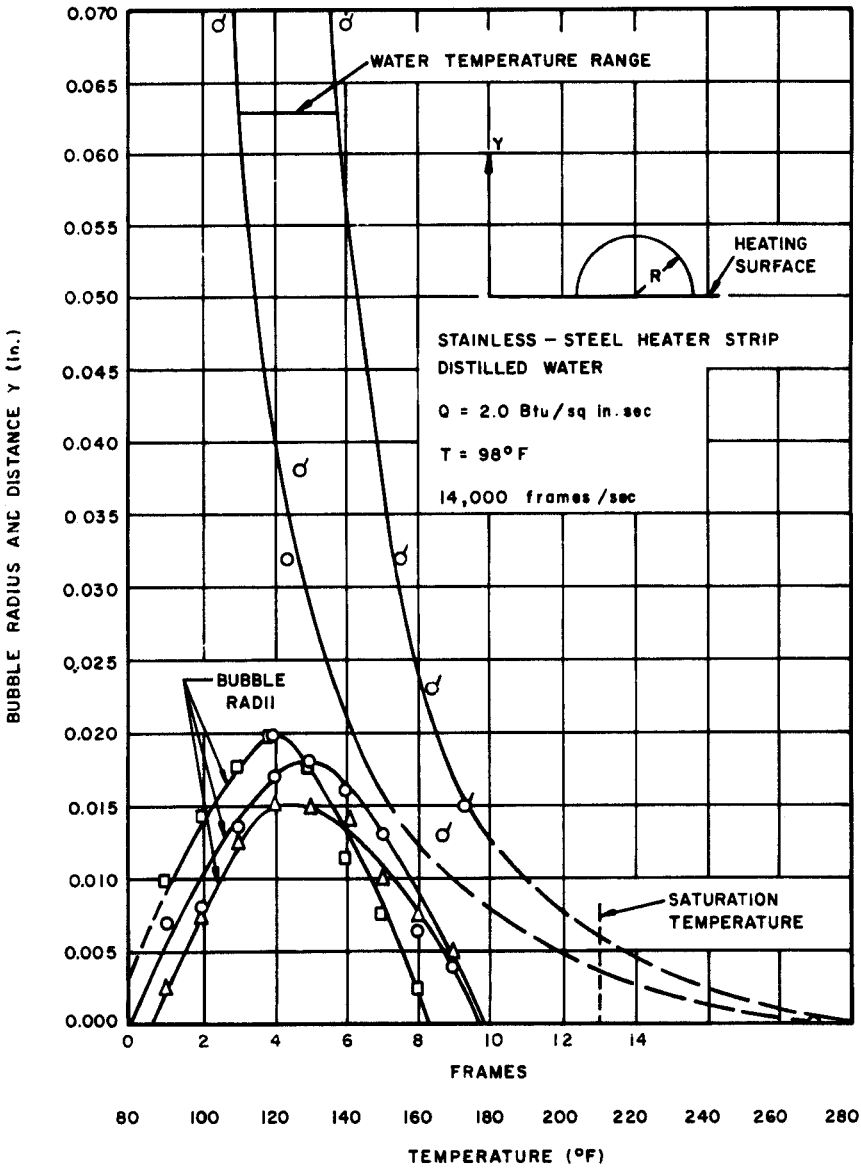


FIG. 18. Temperature distribution in water related to size of hemispherical bubbles (G10).

where the boundary condition $\dot{R} = 0$ when $R = R_m$ has been employed. It will be noted that, in fact, this equation has the desired symmetry, since the sign of $\dot{R}$ does not affect the right-hand side. A further integration of this

equation can be performed numerically. A particularly simple result is obtained if the surface tension term can be neglected, resulting in (L4):

$$\frac{t_m}{R_m} = \left\{\frac{\rho}{6(-\Delta p)}\right\}^{1/2} \frac{\Gamma(1/2)\,\Gamma(5/6)}{\Gamma(4/3)} \tag{106}$$

Bankoff and Mikesell (B11)[10] showed that this equation could be fairly well fitted to the bubble data of Gunther (G9) and of Ellion (E2) (Fig. 19), taken

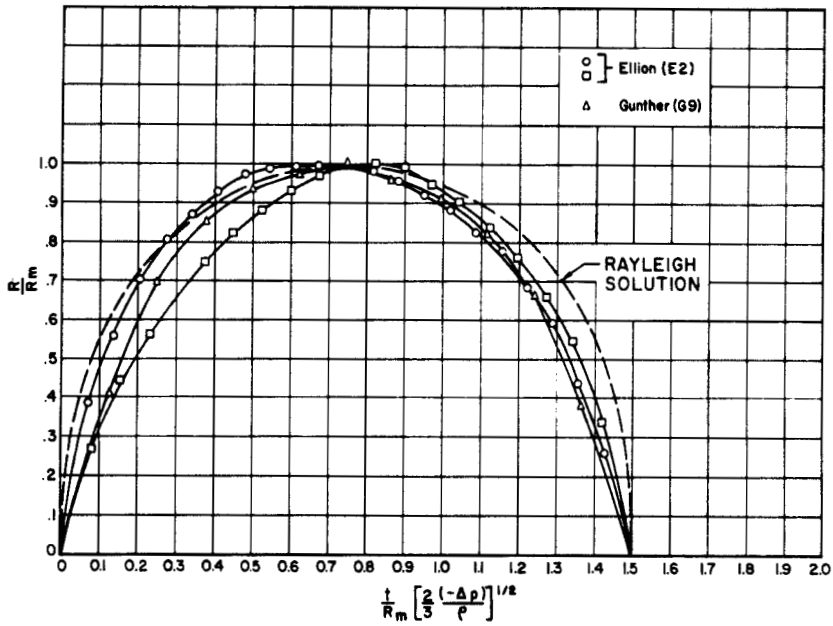


FIG. 19. Bubble growth curves from the data of Gunther (G9) and Ellion (E2) compared with Rayleigh solution, Eq. (106) (B11).

under highly subcooled boiling conditions. This shows that the pressure difference between the bubble interior and the surroundings was nonnegligible, and varied little during the visible lifetime of these bubbles.

Note that at this point no recourse need be made to any theory of energy transport, since the only equation necessary to describe the motion of the fluid is the pressure equation. The calculated pressure difference as a function of subcooling is shown in Fig. 20 from the data of Gunther and Kreith (G10) at a heat flux of 2.75 Btu/(sq in.)(sec) and a superficial liquid velocity of 10 ft/sec past the heating strip. One interpretation of these results is that the liquid surrounding the bubble has been given an initial supply of kinetic

[10] The reader is warned of several misprints in this reference.

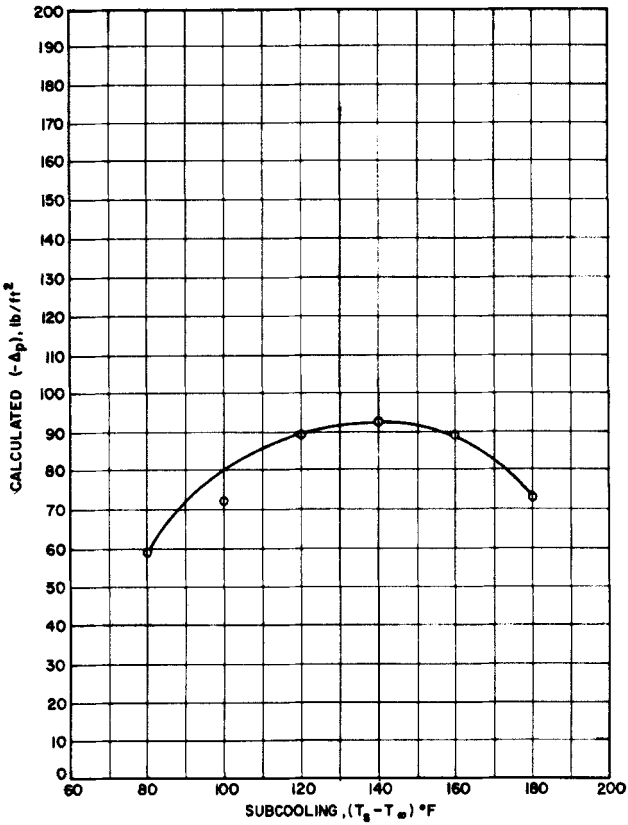


FIG. 20. Calculated pressure difference vs subcooling (B11).

energy, stemming from rapid vaporization of superheated liquid in the thermal boundary layer next to the heating surface. Thereafter, a negative pressure difference tends to slow up bubble growth, and eventually results in collapse. As might be expected, the initial kinetic energy decreases as the bulk temperature, and hence the superheat energy of the wall boundary layer, decreases. This is shown in Fig. 21, based on the same data. Since the pressure within the bubble is below saturation pressure, a good portion of the bubble wall must be below the saturation temperature. A nonequilibrium condition therefore exists, in which a portion of the bubble wall closest to the heating surface is at or above the saturation temperature, while other portions are substantially below this temperature. This implies that appreciable latent heat transport occurs by simultaneous vaporization from the hotter portions of the bubble surface and condensation on the colder regions. As pointed out by Gunther and Kreith (G10), small-scale turbulent diffusion must occur in the

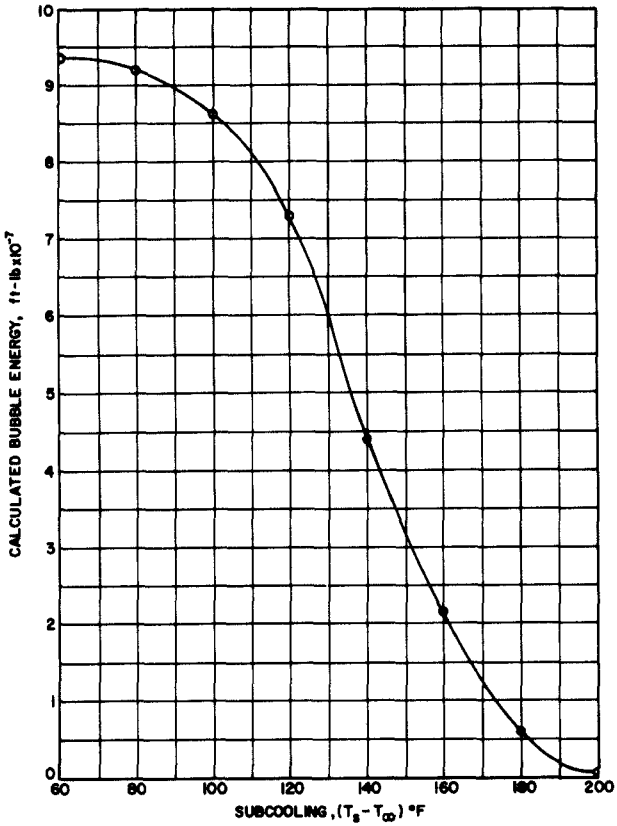


FIG. 21. Calculated initial bubble kinetic energy vs subcooling (B11).

thermal boundary layer at the upper portion of the bubble in order to maintain such temperature differences. That this is, in fact, the situation was demonstrated experimentally by Bankoff and Mason (B9), who measured heat transfer coefficients from an impinging water jet to bubbles formed by injection of steam through a pinhole in a flat surface. Exceptionally high heat transfer coefficients were recorded, the maximum being in excess of $3 \times 10^5$ Btu/(hr)(sq ft)(°F). This is probably as high a heat transfer coefficient as one can find in the engineering literature, and must certainly be related to the striking efficiency of heat transfer in subcooled nucleate boiling.

## B. ZUBER'S MODEL

The relevance of the theories for isolated bubble growth presented above to the problem of the growth of a bubble at a heating surface remains to be

established. In the meantime there is room for, and in fact a need for, phenomenological theories which focus on some hypothesized physical mechanism. By thus constructing a model for the bubble growth, relatively simple expressions can often be deduced from which comparisons with experimental data can be made. It is rare that a completely convincing argument can be made, since usually insufficient experimental evidence is available to verify that the proposed model actually represents all the physics of the problem; nevertheless, such theories can be extremely valuable.

Zuber (Z4) writes for the heat balance on the growing bubble

$$L\rho' \frac{dR}{dt} = b\left[k\frac{T_w - T_s}{(\pi\alpha t)^{1/2}} - q_b\right] \tag{107}$$

where $b$ is a curvature correction factor, and $q_b$, which represents a correction on the initially uniform temperature field heat flux, is identified with the steady-state heat flow from the heating surface to the liquid. Note that the effect of this correction term is to reduce the bubble growth rate compared to the uniform superheat case ($R \propto t^{1/2}$), as noted above. Good agreement between theory and experiment is shown for three bubbles measured by Bankoff and Mikesell (B11), from unpublished film taken by Zmola (Z3), of saturated boiling from a horizontal strip, and also for several bubbles measured by Fritz and Ende (F9).

For subcooled boiling this equation predicts that the maximum radius $R_m$ is reached when

$$(\pi\alpha t_m)^{1/2} = \frac{k\,\Delta T}{q_b}, \qquad \Delta T = T_w - T_s \tag{108}$$

In dimensionless form this yields

$$R/R_m = (t/t_m)^{1/2}[2 - (t/t_m)^{1/2}] \tag{109}$$

where $t_m$ is the time at which the maximum radius is reached. This growth expression is shown to agree with Ellion's data (E2) for subcooled pool boiling. However, it does not work well for the collapse phase. An explanation which is advanced is that in the collapse phase inertial terms dominate, so that the extended Rayleigh equation, Eq. (104), is appropriate. The physical justification is not clear, since the growth time for vapor bubbles from a heating surface is always less than or equal to the collapse time. The maximum bubble diameter is given by

$$\frac{D_m}{X_s} = \frac{\Delta T\, c_p \rho}{L\rho'} \tag{110}$$

where the thickness of the superheated liquid film is given by

$$X_s = \frac{k\,\Delta T}{Q} \tag{111}$$

This is an energy balance stating that the enthalpy of the superheated liquid film contributes, in some constant proportion, to the formation of a bubble which grows on the surface. The similarity to the discussions in the two preceding sections may be noted.

### C. Forster's Model

Forster (F6) solves the same problem by a different approximate method. The temperature profile through the thermal boundary layer next to the heating surface is taken to be exponential. The rather strong assumption is then made that the heat flux through a surface element of the bubble can be equated to the one-dimensional heat flow through the surface of a semi-infinite strip initially at a uniform temperature equal to the local temperature of the thermal boundary layer of the wall before bubble growth began. This ignores the steep initial temperature gradients. Introducing this simplification into the integral heat balance equation for the bubble growth one finds that, for the early asymptotic stage, $R(t) \propto t^{1/2}$, while after the bubble has grown large compared to the thermal boundary layer, $R(t) \propto t^{1/4}$. Qualitatively, this trend is in the direction exhibited by the numerical and analytical solutions (G7, S2, S12).

## V. Miscellaneous Topics

A number of other topics, while highly germane to the general subject of bubble dynamics, are peripheral from the point of view of this review, and hence will be dealt with briefly below. Sufficient references are given in each case to enable the interested reader to pursue the subject further.

### A. Nucleation

In theory it is possible to nucleate bubbles either in the bulk phase or at solid surfaces as a result of statistical density fluctuations. In practice, the theoretical and measured fracture pressures of pure liquids are far in excess of those corresponding to the superheats or supersaturations for vapor or gas bubble nucleation experimentally observed in engineering systems (F2, F7, K1). On the other hand, conditions for homogeneous nucleation become favorable at extremely high superheats in the presence of ionizing radiation (G4, G5). The latter observation led to the introduction of the liquid-hydrogen bubble chamber. A simple explanation of this phenomenon is that the

electrical charges on the bubble surface repel each other, effectively reducing the surface tension. Also, high-energy particles, such as fission fragments, by vaporizing a minute volume of liquid, can induce nucleation under favorable circumstances (H5, N2, S5). More generally, however, the tensile stress at which nucleation is observed is of the order of 1–5 atm, which is far below the theoretical limits of $10^2$–$10^3$ atm. The reduction of this threshold level due to the presence of microscopic roughness elements in the container walls can be shown to be at most by a factor of two or so (B2), so that this possibility can also be ruled out. This means that nucleation in almost all systems of practical importance begins with pre-existing gas or vapor phase, usually trapped in microscopic cavities in the container walls or dust particles. Some theoretical conditions for microscopic grooves or cavities to be effective vapor traps have been deduced (B1, B3, B4), which are essentially of a geometrical nature, depending upon the liquid contact angle, and assuming quasi-static conditions. These give necessary, but not sufficient, conditions for nucleation. A dynamic theory for penetration of liquid into a potential nucleation site remains largely to be developed, although some preliminary work is available (B4). It has been shown that the superheat required to initiate boiling decreases with increasing surface roughness (C5), but the quantitative confirmation of theoretical superheats on the basis of measured surface properties is complicated by the difficulty in obtaining reproducible boiling from particular sites (B13). For this reason some attention has been paid to nucleation from artificial sites (G8, N1, W1). Statistical measurements have also been made of nucleation site densities (C3, G1, G2). Boiling from a liquid–liquid interface has been examined by Viskanta and Lottes (V4) and Otterman (O1), but the results are clouded by the difficulty in obtaining a dust-free interface. By assuming that the nucleation proceeds when the thermal boundary layer thickness at the heating surface reaches some critical fraction of the nucleus radius, the waiting time between bubbles can be calculated (H2, H10). There seems to be considerable evidence of the effects of diffusion of permanent gas into or out of the nucleation cavities, resulting in "aging" of a heating surface in the first few hours of boiling (B13)[11], and the strong influence of

[11] There also appears to be a hysteresis, or time-lag effect, in cycling a heating surface around the nucleation temperature. Presumably this is due to some irreversibility in quenching of formerly active sites. This effect has generally not been taken into account in considering the effect of motion of boiling boundary in the response of boiling channels with subcooled inlet flows to power or flow oscillations. The delayed vaporization resulting from this effect is, in fact, probably the explanation for the sharp "bumping" at times observed in these systems. A dramatic illustration was reported by Zivi *et al.* (Z2), who found that the details of the internal channel construction had a marked effect on the smoothness of the exit void-fraction response to power modulation. A smooth welded channel had a considerably more peaked response than a soldered channel, in accordance with the observation that the solder contained numerous microscopic re-entrant cavities.

prepressurization or of prolonged immersion in promoting resistance to inception of cavitation (H3).

The prediction of the inception of cavitation is, of course, closely related to nucleation theory, but has generally been studied experimentally by modeling with reference to the hydrodynamic flow field (E1, L7, S15). The usual criterion is the Prandtl cavitation number (M6),

$$N_c = \frac{p_\infty - p_c}{\frac{1}{2}\rho u_\infty^2}, \tag{112}$$

which normalizes the critical underpressure at the surface with respect to the dynamic pressure of the free stream. Probably a more successful criterion would be the ratio of the critical underpressure to a characteristic capillary pressure, determined by the surface roughness distribution.

## B. Rapid Heating

A situation of considerable practical concern is the growth of bubbles under rapid heating, such as occurs in fast power excursions in liquid-cooled nuclear reactors. Zwick (Z5) has considered bubble growth in liquids containing strong volume heat sources, by an extension of the perturbation analysis discussed above. It is assumed that the temperature far from the bubble increases linearly: $T_\infty = T_s + bt$, where $t = 0$ corresponds to the instant when the surroundings reach the saturation temperature. The asymptotic phase is extrapolated backwards to zero initial radius, so that $R(0) = 0$. An implicit integral equation for $R(t)$ is then obtained, which is manipulated to give "early" and "late" asymptotic solutions:

$$R \sim \begin{cases} 2\left(\dfrac{3\alpha(t - t_w)}{\pi}\right)^{1/2} N_J, & t \to t_w \\ 6cbN_J\left(\dfrac{\alpha t^3}{7\pi}\right)^{1/2}, & t \to \infty \end{cases} \tag{113}$$

where $t_w$ is a waiting time estimated from the early phase analysis, and $c = 1 - (3/7)[1 - (1/3)\mathrm{B}(3/2, 1/3)] = 0.932$. Although the bubble begins to grow as the square root of time, it eventually increases as $t^{3/2}$. A similar result was obtained by Bankoff (B5) in an analysis of bubble dynamics from an exponentially heated plate.

Vapor formation rates in rapidly heated systems have been measured by Faneuff, McLean, and Scherrer (F1) and Cole (C4) for wires in a stationary liquid pool, and by Johnson *et al.* (J1, J2, T1) for a metal ribbon suspended in a channel flow. Void growth rates in a volume-heated boiling system were studied by Lipkis, Liu, and Zuber (L8). In practice the total vapor volume

depends upon the number of bubbles per cubic centimeter which begin to grow in every small time interval, which in turn depends upon a generally unknown nucleus distribution density function. Zwick (Z5) shows how one can infer this distribution function from measurements of the rate of vapor production in volume boiling through the application of linear transform theory.

### C. Microlayer Vaporization

In 1936 Derjagin (D4) demonstrated the existence of thin liquid films at the base of bubbles attached to a solid surface, which was attributed to the variation of free interfacial energy of very thin films with their thickness. For stationary bubbles these films were of the order of $10^{-5}$ cm thick. Bankoff (B12) called attention to the possibility of the existence of such films at the base of vapor bubbles in nucleate boiling, pointing out that such films would very rapidly evaporate. Moore and Mesler (M7), however, were the first to provide solid experimental confirmation that such microlayers do exist, by measuring the temperature depression of the solid surface directly beneath a number of growing bubbles. The thickness of the liquid film that had to evaporate in order to account for the observed temperature drop was computed to be of the order of $2 \times 10^{-4}$ cm thick. This is of the right order of magnitude, considering the fact that films formed under dynamic conditions would be expected to be thicker than those existing under stationary bubbles. Similar measurements have been made by Hendricks and Sharp (H4).

### D. Other Bubble Properties

A number of other aspects of bubble behavior have received attention. Bubble growth under normal and reduced gravity conditions have been studied by Siegel and co-workers (K2, S9, S10, U1), and by Merte and Clark (M5) in an accelerating system. Bubble behavior in oscillating pressure fields has been analyzed by Houghton (H7) and Plesset and Hsieh (P5, H9). Plesset (P4), in a general review, discusses the stability of collapsing bubbles. Other characteristics of bubbles emanating at heating surfaces, such as mean bubble frequencies, break-off diameters, coalescence frequencies, and nucleation site densities, have been measured in various laboratories (B15, B16, K3, L1, L2, L3, M4, P2, S6, S7, S8). The effect of varying the surface tension in boiling heat transfer has been studied, among others by Myers and co-workers (K6, R2). Bubble parameters in the neighborhood of the critical heat flux have been studied by Cole (C4). Ruckenstein (R3), Chao (C1), and Zavoiskii (Z1) have studied bubble growth when the bubble center is translating with respect to the fluid.

## VI. Concluding Remarks

It is apparent from the preceding survey that, although much has been accomplished in this field, much remains to be done. The theory of isolated bubble growth in a liquid of arbitrary initial temperature and/or concentration distribution is now fairly well established, providing that the boundary layer volume is smaller than the bubble volume. Further research needs to be done on the matching of the quasi-stationary and the thin boundary layer solutions. The theory has to date focused on spherical or hemispherical bubbles, but more frequently bubbles in the shape of ellipsoids or spherical segments are observed growing on surfaces. A solution for these cases, based upon either ellipsoidal or bipolar coordinates, would be helpful. Horvay and Cahn (H6), employing a procedure due to Ivantsov (I1), showed that exact self-similar solutions exhibiting a square root of time dependency exist for a variety of shapes, including paraboloids and ellipsoids, providing that the quasi-stationary assumption is valid. A theoretical examination of the effect of heat transfer from the solid surface after the bubble has entered the asymptotic stage is also needed. Numerical solutions of the problem of two bubbles growing at a surface simultaneously would be helpful in understanding bubble interaction. An interesting and difficult numerical free-boundary problem is the computation of the velocity and temperature fields, and the bubble shape and position, during one complete cycle of bubble growth and departure.

The important advances, however, will be made in the experimental area. Thermocouples and hot wire anemometers of truly small dimensions and of time constants of the order of one microsecond are now becoming commercially available. In order to make a convincing comparison with theory it is necessary to have reasonably accurate measurements of the temperature and velocity fields surrounding the bubbles. Instantaneous as well as time-mean values are of interest. Steps have been taken in this direction in measuring the temperature depression in the solid underneath the bubble (H4, M7, R1). These measurements are quire difficult to make, and a good deal of deductive reasoning has to be employed in any case. It is important, when comparing radius-time curves for bubbles originating on a heating surface with theoretical predictions, that an attempt be made to determine the approximate thermal boundary layer thickness on the heating surface from the data. If, *a priori*, it is assumed that the bubble is initially in a uniform superheat field, much information is lost that could be obtained by finding the assumed nonuniform temperature field which gives the best fit to the data.

Much remains to be done experimentally and theoretically in other aspects of bubble behavior at solid surfaces, such as nucleation, coalescence,

departure, and interaction. These are not simple problems and they promise to tax the ingenuity of investigators for some time.

ACKNOWLEDGMENTS

This work was supported by a grant from the National Science Foundation. Once again, the valuable assistance of Dr. V. K. Pai in assembling and editing this manuscript is acknowledged with thanks. The comments of Professors L. A. Skinner and J. W. Westwater both of whom carefully reviewed the manuscript, were most helpful.

## Nomenclature

$a$ Constant, Eq. (77)

$a_1, a_2, \ldots$ Constants, Eq. (64)

$A$ $=A(T'-T_s)$, linear function of temperature, Eq. (37)

$A_1$ Constant, Eq. (102)

$b$ Constant, Eq. (113), or a curvature correction factor, Eq. (107)

$b_0, b_1, b_2,$ Constants, Eq. (68)

$B(p, q)$ Beta function

$c$ Constant, Eq. (113)

$c_p$ Specific heat at constant pressure

$C$ Concentration

$d_0, d_1,$ Functions of $s$, Eq. (69)

$D$ Bubble diameter

$D_m$ Maximum bubble diameter

$D$ Mass diffusivity

$f(m)$ Initial temperature distribution in liquid, Eq. (71)

$F(\zeta)$ $=\partial^2 U(0, \zeta)/\partial m^2$, Eq. (28)

$\mathcal{F}(t)$ Function of time, Eq. (1)

$g(r)$ Initial temperature distribution, Eq. (11)

$g(m)$ $=\dfrac{f(m)-T_s}{f(0)-T_s}$, dimensionless initial temperature distribution, Eq. (71)

$g[R(\zeta)]$ Function defined in Eq. (45)

$h(r)$ Initial concentration distribution in liquid, Eq. (12)

$\tilde{h}$ Heat transfer coefficient from heating surface to vapor bubble through its base area

$I$ Current density

$j$ Iteration index

$k$ Thermal conductivity

$k_1$ $=\beta'/I^{-1/3}$

$k_H$ Henry's Law constant

$K$ Constant, Eq. (94)

$K_1$ $=\left(\dfrac{2\sigma}{\rho R_0^3}\right)^{1/2}$, Eq. (39c)

$K_2$ Constant, Eq. (41)

$l$ Characteristic length or initial thermal boundary layer thickness

$L$ Latent heat of vaporization

$m$ $=\frac{1}{3}[r^3 - R^3(t)]$, position variable

$M$ Molecular weight

$N_c$ Prandtl cavitation number, Eq. (112)

$N_J$ $=\dfrac{\rho c_p(T_{b0} - T_s)}{\rho' L}$, dimensionless (Jakob number)

$N_J'$ $=\dfrac{C_\infty - C_s}{C_g}$, dimensionless concentration

$N'J'$ $=\dfrac{k\,\Delta T}{\rho' L\alpha}$, generalized Jakob number, Eq. (88)

$p$ Pressure

$p_r$ Reduced pressure

$p_v$ Vapor pressure of liquid

$q_b$ Correction term on the initial uniform temperature field, Eq. (107)

$Q$ Heat flux density

$Q'$ Instantaneous local rate of concentration increase, Eq. (9)

$r$ Radial position

$R(t)$ Bubble radius

$R_g$ Universal gas constant
$R_i$ Radius of isothermal vapor bubble, Eq. (94)
$R_m$ Maximum bubble radius
$R_0$ Initial bubble radius
$R_1$ Bubble radius at the commencement of asymptotic growth
$R^*$ $= R^3/R_0^3$, dimensionless, Eq. (39a)
$\mathscr{R}$ $= R/l$, dimensionless bubble radius, Eq. (73)
$s$ $= y/R$, dimensionless radius
$t$ Time
$t_c$ Time at which bubble collapses to zero radius
$t_m$ Time at which maximum bubble radius is attained
$t_w$ Waiting period between bubbles
$T$ Temperature
$T_{b0}$ $= f(0)$, bubble wall temperature; for uniform superheat, $T_{b0} = T_\infty$; for bubbles originating at the heating surface, $T_{b0} \approx T_w$
$T_e$ Temperature excess, $(T - T_\infty)$, Eq. (24)
$u(r, t)$ Liquid velocity, Eq. (1)
$U$ $= \int_0^m T_e(m, t)\, dm$, temperature potential function, Eq. (24)
$U_0, U_1, \ldots$ Perturbation functions of $U$
$V$ $= R^3(t)$, Eq. (53)
$V_0, V_1, \ldots$ Perturbation functions of $V$
$x$ Distance normal to the wall; or dummy variable in integration
$X_s$ Thickness of superheated liquid film, Eq. (110)
$y$ $= (r - R)$, position variable
$y_A$ Mass fraction of volatile component $A$
$z$ Dummy variable

GREEK LETTERS

$\alpha$ Thermal diffusivity
$\beta$ $= R/(\alpha t)^{1/2}$, growth constant
$\beta'$ $= \beta/2$
$\gamma$ Accommodation coefficient
$\Gamma$ Gamma function
$\delta$ Thickness of thermal boundary layer, Eq. (98)
$\delta_1$ Small displacement from equilibrium bubble radius, Eq. (10)
$\Delta$ Standard notation for difference
$\varepsilon$ $= [1 - \langle\rho'\rangle/\rho]$, dimensionless term
$\zeta$ $= \int_0^t R^4(t')\, dt'$, time variable, Eq. (23)
$\zeta_1$ $= \frac{\alpha}{l^2} \int_0^t \mathscr{R}^4(t')\, dt'$, time variable, Eq. (73)
$\zeta^*$ $= K_1\zeta/R_0^4$, time variable, Eq. (39b)
$\eta$ $= r/(\alpha t)^{1/2}$, Boltzmann transformation variable
$\theta$ Spherical polar coordinate
$\theta(\mathbf{r}, t)$ $= (T - T_\infty)/(T_s - T_\infty)$, dimensionless temperature, Eq. (15)
$\Theta(m, t)$ Averaged temperature excess, defined in Eq. (82)
$\kappa$ Effective surface dilational viscosity
$\mu$ Viscosity
$\nu$ Kinematic viscosity
$\rho$ Density
$\langle\rho'\rangle$ Time-averaged vapor density
$\sigma$ Surface tension
$\tau$ $= \frac{\alpha t}{l^2}$, dimensionless time, Eq. (91)
$\varphi$ Contact angle; or spherical polar coordinate
$\varphi(m)$ $= \partial U_0'(m, 0)/\partial m$, Eq. (46)
$\varphi_b$ $= \frac{\sin^2 \varphi}{4}$, base factor, Eq. (97)
$\varphi_c$ Curvature factor, Eq. (97)
$\varphi_s$ $= \frac{1 + \cos \varphi}{2}$, surface factor, Eq. (97)

$\varphi_v$ $= [2 + \cos\varphi(2 + \sin^2\varphi)]/4$, volume factor, Eq. (97)

$\Phi$ $= N_J'/(1 - C_s/\rho)$, constant, Fig. (15)

$\Phi_3(\eta)$ Function defined in Eq. (16)

$\chi(\beta)$ Function defined in Eq. (18)

$\psi(z)$ Function defined in Eq. (92)

$\omega$ $= (T_w - T_\infty)/(T_w - T_s)$, dimensionless temperature

SUBSCRIPTS (UNLESS OTHERWISE NOTED)

$A$ Volatile component $A$

$b$ Condition within the bubble

$g$ Gas

$m$ Maximum

$s$ Saturated

$v$ Vapor

$w$ Wall of the heating surface

$\infty$ Condition at infinity

SUPERSCRIPTS (UNLESS OTHERWISE NOTED)

$'$ Vapor phase

$-$ Average

$.$ Time derivative

## REFERENCES


B1. Bankoff, S. G., *J. Phys. Chem.* **60**, 952 (1956).

B2. Bankoff, S. G., *J. Heat Transfer* **79**, 735 (1957).

B3. Bankoff, S. G., *A.I.Ch.E. (Am. Inst. Chem. Engrs.) J.* **4**, 24 (1958).

B4. Bankoff, S. G., *Chem. Eng. Progr., Symp. Ser.* **55**, No. 29, 87 (1959).

B5. Bankoff, S. G., *Ind. Eng. Chem., Fundamentals* **1**, 257 (1962).

B6. Bankoff, S. G., *A.I.Ch.E. (Am. Inst. Chem. Engrs.) J.* **8**, 63 (1962).

B7. Bankoff, S. G., *Appl. Sci. Res.* **A12**, 567 (1963).

B8. Bankoff, S. G., *Advan. Chem. Eng.* **5**, 75–150 (1964).

B9. Bankoff, S. G., and Mason, J. P., *A.I.Ch.E. (Am. Inst. Chem. Engrs.) J.* **8**, 30 (1962).

B10. Bankoff, S. G., and Mikesell, R. D., *Am. Soc. Mech. Engrs., Paper* **58-A-105** (1958).

B11. Bankoff, S. G., and Mikesell, R. D., *Chem. Eng. Progr., Symp. Ser.* **55**, No. 29, 95 (1959).

B12. Bankoff, S. G., Colahan, W. J., Jr., and Bartz, D. R., "Summary on Conference on Bubble Dynamics and Boiling Heat Transfer." Jet Propulsion Lab., Cal. Inst. Tech., Pasadena, California, Memo. No. 20-137, 1956.

B13. Bankoff, S. G., Hajjar, A. J., and McGlothin, B. B., Jr., *J. Appl. Phys.* **29**, 1739 (1958).

B14. Barlow, E. J., and Langlois, W. E., *IBM J. Res. Develop.* **6**, 329 (1962).

B15. Behar, M., *Houille Blanche* **18**, 692 (1963).

B16. Behar, M., and Semeria, R., *Compt. Rend.* **255**, 1331 (1962).

B17. Benjamin, J. E., and Westwater, J. W., "International Developments in Heat Transfer," Part II, p. 212. Am. Soc. Mech. Engrs., New York, 1961.

B18. Benjamin, J. E., and Westwater, J. W., *Proc. 5th Intern. Congr. High Speed Phot., Washington, 1960 D.C.*, Soc. Motion Picture and Television Engrs., New York, p. 290 (1962).

B19. Birkhoff, G., Margulies, R. S., and Horning, W. A., *Phys. Fluids* **1**, 201 (1958).

B20. Boley, B. A., *J. Math. Phys.* **40**, 300 (1961).

B21. Boltzmann, L., *Ann. Physik* [3] **53**, 959 (1894).

B22. Bosnjakovic, F., *Tech. Mech. Thermo-Dynam., Berlin* **1**, 358 (1930).

B23. Brandstaetter, F., *Österr. Akad. Wiss.* **161**, 107 (1952); cf. Houghton, G., Ritchie, P. D., and Thomson, J. A., *Chem. Eng. Sci.* **17**, 221 (1962).

B24. Bruijn, P. J., *Physica* **26**, 326 (1960).

B25. Buehl, W. M., and Westwater, J. W., *A.I.Ch.E. (Am. Inst. Chem. Engrs.) J.* (submitted for publication).

B26. Bumpus, C., Spiegler, P., and Norman, A., *Trans. Am. Nucl. Soc.* **4**, 70 (1961).

C1. Chao, B. T., *Phys. Fluids* **5**, 69 (1962).

C2. Cichelli, M. T., and Bonilla, C. F., *Trans. Am. Inst. Chem. Engrs.* **41**, 755 (1945).
C3. Clark, H. B., Strenge, P. S., and Westwater, J. W., *Chem. Eng. Progr., Symp. Ser.* **55**, No. 29, 103 (1959).
C4. Cole, R., *A.I.Ch.E. (Am. Inst. Chem. Engrs.) J.* **6**, 533 (1960).
C5. Corty, C., and Foust, A. S., *Chem. Eng. Progr., Symp. Ser.* **51**, No. 17, 1 (1955).
D1. Darby, R., *Chem. Eng. Sci.* **19**, 39 (1964).
D2. Dergarabedian, P., *J. Appl. Mech.* **20**, 537 (1953).
D3. Dergarabedian, P., *J. Fluid Mech.* **9**, 39 (1960).
D4. Derjagin, B., *Acta Phys.-chim. URSS* **5**, 1 (1936); **10**, 333 (1937).
D5. Doremus, R. H., *J. Am. Ceram. Soc.* **43**, 655 (1960).
D6. Dougherty, D. E., and Rubin, H. H., *Proc. Heat Transfer Fluid Mech. Inst., 1963* p. 222. Stanford Univ. Press, Stanford, California, 1963.
E1. Eisenberg, P., and Tulin, M. P., "Handbook of Fluid Dynamics" (V. L. Streeter, ed.), Section 12. McGraw-Hill, New York, 1961.
E2. Ellion, M. E., "A Study of the Mechanism of Boiling Heat Transfer." Jet Propulsion Lab., Cal. Inst. Tech., Pasadena, California, Memo No. 20-88, 1954.
E3. Epstein, P. E., and Plesset, M. S., *J. Chem. Phys.* **18**, 1505 (1950).
F1. Faneuff, C. E., McLean, E. A., and Scherrer, V. E., *J. Appl. Phys.* **29**, 80 (1958).
F2. Fisher, J. C., *J. Appl. Phys.* **19**, 1062 (1948).
F3. Flatt, H. P., *Trans. Am. Nucl. Soc.* **1**, 48 (1958).
F4. Forster, H. K., *A.I.Ch.E. (Am. Inst. Chem. Engrs.) J.* **3**, 535 (1957).
F5. Forster, H. K., and Zuber, N., *J. Appl. Phys.* **25**, 474 (1954).
F6. Forster, K. E., *Phys. Fluids* **4**, 448 (1961).
F7. Frenkel, J., "Kinetic Theory of Liquids," Dover, New York, 1955.
F8. Fricke, R., *Z. Physik. Chem. (Leipzig)* **104**, 363 (1923).
F9. Fritz, W., and Ende, W., *Phys. Z.* **37**, 391 (1936).
G1. Gaertner, R. F., *Chem. Eng. Progr., Symp. Ser.* **59**, No. 41, 52 (1963).
G2. Gaertner, R. F., and Westwater, J. W., *Chem. Eng. Progr., Symp. Ser.* **55**, No. 30. 39 (1959).
G3. Glas, J. P., and Westwater, J. W., *Intern. J. Heat Mass Transfer* **7**, 1427 (1964).
G4. Glaser, D. A., *Phys. Rev.* **87**, 665 (1952).
G5. Glaser, D. A., *Phys. Rev.* **91**, 762 (1953).
G6. Greene, C. H., and Gaffney, R. F., *J. Am. Ceram. Soc.* **42**, 271 (1959).
G7. Griffith, P., *J. Heat Transfer* **80**, 721 (1958).
G8. Griffith, P., and Wallis, J. D., *Chem. Engr. Progr., Symp. Ser.* **55**, No. 30, 49 (1959).
G9. Gunther, F. C., "Photographic Study of Surface Boiling Heat Transfer to Water with Forced Convection." Jet Propulsion Lab., Cal. Inst. Tech., Pasadena, California, Progr. Rept. No. 4-75, 1950.
G10. Gunther, F. C., and Kreith, F., "Photographic Study of Bubble Formation in Heat Transfer to Subcooled Water." Jet Propulsion Lab., Cal. Inst. Tech., Pasadena, California, Progr. Rept. No. 4-120, 1950.
H1. Hadamard, J., "Lectures on Cauchy's Problem in Linear Partial Differential Equations." Dover, New York, 1952.
H2. Han, C. Y., and Griffith, P., "Mechanism of Heat Transfer in Nucleate Pool Boiling." Div. of Sponsored Res., Mass. Inst. Tech., Cambridge, Massachusetts, Rept. No. 7673-19, 1962.
H3. Harvey, E. N., McElroy, W. D., and Whiteley, A. H., *J. Appl. Phys.* **18**, 162 (1947).
H4. Hendricks, R. C., and Sharp, R. R., *NASA, Tech. Note* **TN D-2290** (1964).
H5. Hetrick, D. L., and Gamble, D. P., *Trans. Am. Nucl. Soc.* **1**, 48 (1958).
H6. Horvay, G., and Cahn, J. W., *Acta Met.* **9**, 695 (1961).

H7. Houghton, G., *J. Acoust. Soc. Am.* **35**, 1387 (1963).
H8. Houghton, G., Ritchie, P. D., and Thomson, J. A., *Chem. Eng. Sci.* **17**, 221 (1962).
H9. Hsieh, D., and Plesset, M. S., *Phys. Fluids* **4**, 970 (1961).
H10. Hsu, Y. Y., *J. Heat Transfer* **84**, 207 (1962).
I1. Ivantsov, G. P., *Dokl. Akad. Nauk SSSR* **58**, 567 (1947); (Mathematical Physics) (transl. by G. Horvay), Rept. No. 60-RL-(2511M). G.E. Res. Lab., Schenectady, New York, 1960.
J1. Johnson, H. A., Schrock, V. E., Fabic, S., and Selph, F. B., "Transient Boiling Heat Transfer and Void Volume Production in Channel Flow." Reactor Heat Transients Res., Univ. of Calif., Berkeley, California, SAN-1007, TID-4500, 1963.
J2. Johnson, H. A., Schrock, V. E., Selph, F. B., Lienhard, J. H., and Rosztoczy, Z. R., "International Developments in Heat Transfer," Part II, p. 244. Am. Soc. Mech. Engrs., New York, 1961.
K1. Kenrick, F. B., Gilbert, C. S., and Wismer, K. L., *J. Phys. Chem.* **28**, 1297 (1924).
K2. Keshock, E. G., and Siegel, R., *NASA, Tech. Note* TN- **D-2299** (1964).
K3. Kirby, D. B., and Westwater, J. W., *Chem. Eng. Sci.* **18**, 469 (1963).
K4. Kirkaldy, J. J., *Can. J. Phys.* **36**, 446 (1958).
K5. Kolodner, I., *Commun. Pure Appl. Math.* **9**, 1 (1956).
K6. Kurihara, H. M., and Myers, J. E., *A.I.Ch.E. (Am. Inst. Chem. Engrs.) J.* **6**, 83 (1960).
L1. Labuntsov, D. A., *Teploenerg.* **12**, 19 (1959).
L2. Labuntsov, D. A., *Inzh.-Fiz. Zh., Akad. Nauk Belorussk. SSR* **6**, 33 (1963); cf. *Chem. Abstr.* **59**, 8146g (1963).
L3. Labuntsov, D. A., Kol'chugin, B. A., Golovin, V. S., Zakharova, E. A., and Vladimirova, L. N., *Tepl. Vysokih Temp. Akad. Nauk SSSR* **2**, 446 (1964); cf. Chem. Abstr. **61**, 12964b (1964).
L4. Lamb, G., "Hydrodynamics." Dover, New York, 1949.
L5. Langlois, W. E., *J. Fluid Mech.* **15**, 111 (1963).
L6. Liebermann, L., *J. Appl. Phys.* **28**, 205 (1957).
L7. Lienhard, J. H., "A Study of the Dynamics and Thermodynamics of Liquid-Gas-Vapor Bubbles." Washington State Inst. of Technology, Pullman, Washington, Bull. No. 266, 1964.
L8. Lipkis, R. P., Liu, C., and Zuber, N., *Chem. Eng. Progr., Symp. Ser.* **52**, No. 18, 105 (1956).
M1. Ma, J. T., and Wang, P. K., *IBM J. Res. Develop.* **6**, 472 (1962).
M2. Mache, M., *Wien. Akad.* **138**, 529 (1929); cf. Houghton, G., Ritchie, P. D., and Thomson, J. A., *Chem. Eng. Sci.* **17**, 221 (1962).
M3. Manley, D. M. J. P., *Brit. J. Appl. Phys.* **11**, 38 (1960).
M4. McFadden, P. W., and Grassmann, P., *Intern. J. Heat Mass Transfer* **5**, 169 (1962).
M5. Merte, H., Jr., and Clark, J. A., *J. Heat Transfer* **83**, 233 (1961).
M6. Milne-Thomson, L. M., "Theoretical Hydrodynamics." Macmillan, New York, 1960.
M7. Moore, F. D., and Mesler, R. B., *A.I.Ch.E. (Am. Inst. Chem. Engrs.) J.* **7**, 620 (1961).
M8. Morse, P. M., and Feshbach, H., "Methods of Theoretical Physics," Vol. 1. McGraw-Hill, New York, 1953.
N1. Nickelson, R. L., and Preckshot, G. W., *J. Chem. Eng. Data* **5**, 310 (1960).
N2. Norman, A., and Spiegler, P., *Nucl. Sci. Eng.* **16**, 213 (1963).
O1. Otterman, B., *Proc. Heat Transfer Fluid Mech. Inst., 1962* p. 185. Stanford Univ. Press, Stanford, California, 1962.
P1. Patten, T. D., "Some Characteristics of Nucleate Boiling of Water at Sub-atmospheric Pressures." Thermodynamics and Fluid Mech. Convention, Inst. of Mech. Engrs., Cambridge, England, Paper No. 9, 1964.

P2. Perkins, A. S., and Westwater, J. W., *A.I.Ch.E. (Am. Inst. Chem. Engrs.) J.* **2**, 471 (1956).
P3. Plesset, M. S., *J. Appl. Mech.* **16**, 277 (1949).
P4. Plesset, M. S., "Cavitation in Real Liquids" (R. Davies, ed.), pp. 1–17. Elsevier, Amsterdam, 1964.
P5. Plesset, M. S., and Hsieh, D., *Phys. Fluids* **3**, 882 (1960).
P6. Plesset, M. S., and Zwick, S. A., *J. Appl. Phys.* **23**, 95 (1952).
P7. Plesset, M. S., and Zwick, S. A., *J. Appl. Phys.* **25**, 493 (1954).
P8. Poritsky, H., *Proc. 1st U.S. Natl. Congr. Appl. Mech.* **1**, 813 (1951).
R1. Rogers, T. F., and Mesler, R. B., *A.I.Ch.E. (Am. Inst. Chem. Engrs.) J.* **10**, 656 (1964).
R2. Roll, J. B., and Myers, J. E., *A.I.Ch.E. (Am. Inst. Chem. Engrs.) J.* **10**, 530 (1964).
R3. Ruckenstein, E., *Chem. Eng. Sci.* **10**, 22 (1959).
S1. Savic, P., *Natl. Res. Council Can., Rept.* **MR-37** (1958).
S2. Savic, P., and Gosnell, J. W., *Can. J. Chem. Eng.* **40**, 238 (1962).
S3. Scriven, L. E., *Chem. Eng. Sci.* **10**, 1 (1959).
S4. Scriven, L. E., *Chem. Eng. Sci.* **17**, 55 (1962).
S5. Seitz, P., *Phys. Fluids* **1**, 2 (1958).
S6. Semeria, R. L., "An Experimental Study of the Characteristics of Vapor Bubbles." Symp. on Two-Phase Fluid Flow, Inst. Mech. Engrs., London, Paper No. 7, 1962.
S7. Semeria, R., *Houille Blanche* **18**, 679 (1963).
S8. Semeria, R., *Compt. Rend.* **256**, 1227 (1963).
S9. Siegel, R., and Keshock, E. G., *A.I.Ch.E. (Am. Inst. Chem. Engrs.) J.* **10**, 509 (1964).
S10. Siegel, R., and Usiskin, C. M., *J. Heat Transfer* **81**, 230 (1959).
S11. Skinner, L. A., Ph.D. Thesis, Northwestern Univ., Evanston, Illinois, 1963.
S12. Skinner, L. A., and Bankoff, S. G., *Phys. Fluids* **7**, 1 (1964).
S13. Skinner, L. A., and Bankoff, S. G., *Phys. Fluids* **7**, 643 (1964).
S13a. Skinner, L. A., and Bankoff, S. G., *Phys. Fluids* **8**, 1417 (1965).
S13b. Skinner, L. A., personal communication (1965).
S14. Staniszewski, B. E., "Nucleate Boiling Bubble Growth and Departure." Div. of Sponsored Res., Mass. Inst. Tech., Cambridge, Massachusetts, Tech. Rept. No. 16, 1959.
S15. Strasberg, M., "The Influence of Air-filled Nuclei on Cavitation Inception." David Taylor Model Basin, Navy Dept., Rept. No. 1078, 1957.
S16. Strenge, P. H., Orell, A., and Westwater, J. W., *A.I.Ch.E. (Am. Inst. Chem. Engrs.) J.* **7**, 578 (1961).
T1. Tien, C. L., Schrock, V. E., and Johnson, H. A., "On the Prediction of Void Volume in Transient Satd. Pool Boiling." Reactor Heat Transients Res., Univ. of Calif., Berkeley, California, SAN-1004, TID-4500, 1962.
U1. Usiskin, C. M., and Siegel, R., *J. Heat Transfer* **83**, 243 (1961).
V1. Van Wijk, W. R., *Dechema Monograph.* **28**, 63 (1956).
V2. Van Wijk, W. R., and Van Stralen, S. J. D., *Physica* **28**, 150 (1962).
V3. Van Wijk, W. R., Vos, A. S., and Van Stralen, S. J. D., *Chem. Eng. Sci.* **5**, 68 (1956).
V4. Viskanta, R., and Lottes, P. A., *Proc. Heat Transfer Fluid Mech. Inst., 1962* p. 171. Stanford Univ. Press, Stanford, California, 1962.
V5. Vos, A. S., and Van Stralen, S. J. D., *Chem. Eng. Sci.* **5**, 50 (1956).
W1. Wei, C. C., and Preckshot, G. W., *Chem. Eng. Sci.* **19**, 838 (1964).
W2. Westerheide, D. E., and Westwater, J. W., *A.I.Ch.E. (Am. Inst. Chem. Engrs.) J.* **7**, 357 (1961).
W3. Westwater, J. W., *in* "Cavitation in Real Liquids" (R. Davies, ed.), pp. 34–54 Elsevier, Amsterdam, 1964.

W4. Wyllie, G., *Proc. Roy. Soc.* (*London*) **A197**, 383 (1949).
Y1. Yang, W., and Clark, J. A., *J. Heat Transfer* **86**, 207 (1964).
Z1. Zavoiskii, V. K., *Soviet J. At. Energy* (*English Transl.*) **10**, 272 (1961).
Z2. Zivi, S. M., Wright, R. W., and Yeh, G. C. K., "Kinetic Studies of Heterogeneous Water Reactors." Space Tech. Labs., Redondo Beach, California, STL 6212, 1962.
Z3. Zmola, P. C., Ph.D. Thesis, Purdue University, Lafayette, Indiana, 1950.
Z4. Zuber, N., *Intern. J. Heat Mass Transfer* **2**, 83 (1961).
Z5. Zwick, S. A., *Phys. Fluids* **3**, 685 (1960).
Z6. Zwick, S. A., and Plesset, M. S., *J. Math. Phys.* **33**, 308 (1955).